MODELING OF THE ENERGY REQUIREMENTS OF A NON-ROW SENSITIVE CORN HEADER FOR A PULL-TYPE FORAGE HARVESTER

A Thesis Submitted to the
College of Graduate Studies and Research
in Partial Fulfilment of the Requirements
for the Degree of Master of Science in the
Department of Agricultural and Bioresource Engineering

University of Saskatchewan
Saskatoon
Saskatchewan

By
Philippe Nieuwenhof

PERMISSION TO USE

In presenting this thesis in partial fulfillment of the requirements for a degree of Master of Science from the University of Saskatchewan, I agree that the libraries of this University may make it freely available for inspection. I further agree that permission for copying this thesis in any manner, in whole or in part for scholarly purposes may be granted by the professor who supervised my thesis work or, in his absence, by the Head of the Department or the Dean of the College in which my thesis work was done. Copying or publication or use of this thesis or parts thereof for financial gain without the author's written permission is prohibited. It is understood that due recognition shall be given to the author and to the University of Saskatchewan for any scholarly use of material contained in this thesis.

Requests for permission to copy or to make other use of material in this thesis in whole or in part should be addressed to:

Head of the Department of Agricultural and Bioresource Engineering

University of Saskatchewan
57 Campus Drive
Saskatoon, SK. Canada
S7N 5A9

ABSTRACT

With the constant diversification of cropping systems and the constant increase in farm size, new trends are observed for agricultural machinery. The increase in size of the machinery and the increasing number of contractors has opened the market to self-propelled forage harvesters equipped with headers that can harvest row crops in any direction, at any spacing. High-capacity pull-type forage harvesters are also in demand but no commercial model offers non-row sensitive corn headers. The objectives of this research were to collect data and develop models of specific energy requirements for a prototype non-row sensitive corn header. The ability to better understand the processes involved during the harvesting and the modeling of these allowed the formulation of recommendations to reduce the loads on the harvester and propelling tractor.

Three sets of experiments were performed. The first experiment consisted of measuring specific energy requirements of a non-row sensitive header, in field conditions, and to compare them with a conventional header. The prototype tested was found to require approximately twice the power than a conventional header of the same width, mostly due to high no-load power. Some properties of corn stalk required for the modeling of the energy needs, that were not available in literature, were measured in the laboratory. Those include the cutting energy with a specific knife configuration used on the prototype header and the crushing resistance of corn stalk. Two knife designs were compared for required cutting energy and found not to be significantly different with values of 0.054 J/mm^2 of stalk cross-section area and 0.063 J/mm^2. An average crushing resistance of 6.5 N per percent of relative deformation was measured.

Three mathematical models were developed and validated with experimental data to predict and understand the specific energy needs of the non-row sensitive header. An analytical model was developed based on the analysis of the processes involved in the harvesting. A regression model was developed based on throughput and header speed and a general model suggested in literature was also validated with the data. All three models were fitted with coefficient of correlation between 0.88 to 0.90.

ACKNOWLEDGEMENTS

I would like to acknowledge the very generous support, confidence and insights I have received from my supervisor Dr. Martin Roberge without which this work would not have been possible and been so instructive. I would also like to thank the members of my committee, Dr. Claude Laguë and Dr. Trever Crowe.

This project was made possible by the work of Benoît Lamarche and the generous time and support of Dion Machineries Inc., allowing me to gain experience within an industry environment.

Finally, I would like to mention the generous financial support of the *Fond de Recherche sur la Nature et les Technologies* which allowed me, combined with the financial support of the University of Saskatchewan and the Department of Agricultural and Bioresource Engineering, to pursue full-time graduate studies in a pleasant environment.

DEDICATION

Je dédie ce document, mais surtout le travail et le cheminement qu'il représente, à mes parents; pour m'avoir élevé dans un environnement agricole riche en opportunités d'apprentissage et de découverte; pour m'avoir enseigné la participation, l'implication, la patience, l'effort et la passion du travail; pour tous les choix et sacrifices qu'ils ont fait pour faciliter mes études et leur support inconditionnel dans mes démarches personnelles et éducationnelles.

I dedicate this document but especially the work it represents, to my parents: for raising me in a rural environment rich in opportunities to learn and discover; for teaching me participation, involvement, patience, effort and a passion for work; for all he choices and sacrifices they made to facilitate my studies and their unconditional support for my personal and educational endeavours.

TABLE OF CONTENTS

LIST OF FIGURES

LIST OF TABLES

LIST OF ABBREVIATIONS

3-R:	three row (header)
A:	area
ANCOVA:	analysis of covariance
ANOVA:	analysis of variance
AVGBSE:	average blower specific energy
AVGHSE:	average header specific energy
b:	abscise of linear function
C :	constant
C_0:	no-load power
C_1:	constant
CV:	coefficient of variation
d :	stalk diameter
D:	major diameter
D_{equ}:	equivalent diameter
df:	degrees of freedom
DM:	dry matter
e :	experimental error
E:	modulus of elasticity
E_{cut}:	cutting energy
E_{end}:	ending energy
E_{loss}:	energy loss
E_{start} :	starting energy
F_c:	cutting force
F_S:	stalk deflecting strength
g:	gravitational acceleration
h:	header treatment effect
H_0:	null hypothesis
H_1:	hypothesis
I:	moment of inertia
K:	stalk cross–section deformation constant
KE:	kinetic energy
L:	chain conveying length
L_k :	knife tip radius
m:	mass of the pendulum
MAXHSE:	maximum header specific energy
MAXBSE:	maximum blower specific energy
MC :	moisture content on a wet basis
MS:	mean squares
m_l:	linear mass
N:	number of rows harvested per drum
NRS:	non-row sensitive (header)
v_{cr}:	critical velocity
p:	probability
P :	power

$\dot{p}$:	harvesting rate
P_0:	no-load power
P_c:	cutting power
P_{cv}:	conveying power
P_g:	gathering power
PE:	potential energy
Pop:	corn plant
PTFH:	pull-type forage harvester
PTO:	Power take-off
Q:	throughput
R^2:	coefficient of multiple determination
rpm:	revolutions per minute
s:	spacing between conveying chains
S:	corn row spacing
SE:	specific energy
SPFH:	self-propelled forage harvester
t:	time
T:	point load
V:	harvesting speed
y_c:	deflection at center of beam
w.b.:	wet basis
W_{path}:	work circular path
β:	regression coefficient
δ:	average deformation of stalks
ϕ:	angular position
λ :	ratio of the tangential velocity to the forward velocity
θ:	angular position
θ_0 :	starting position
θ_{start}:	starting angle
θ_{end} :	ending angle
μ:	friction coefficient
μ_o:	overall friction coefficient
ω:	angular velocity

1. INTRODUCTION

Corn (*Zea Mays*) is a major crop in North America, Western Europe and some regions of Africa. It is used as a main feed source by many livestock productions such as swine, beef and dairy. Either the grain or the whole plant is harvested to feed the animals. Whole plant silage is a very common source of feed for dairy and beef production. Corn production extends through a large portion of the agricultural regions, but it is viable predominantly in Eastern Canada and in the US from the Eastern coast to the Midwest. From the 1.29 million hectares and 32 million hectares of corn harvested in Canada and the USA, respectively, in 2000, 15.6% (Canada) and 8.4% (USA) were harvested for silage for a total production of 98.4 Tg (National Agricultural Statistic Service, 2002; Statistics Canada, 2002). Corn silage is a high-energy feed, well suited for beef fattening and easily incorporated in total mix rations for dairy cows.

Corn varieties used for silage are more often hybrids, specifically developed for that purpose, producing large quantities of dry matter per land area, with less emphasis on grain production. A rule of thumb to detect the ideal time of harvest for best nutritive value and moisture content is to harvest when the milk line is located between 1/3 and 2/3 of the grain kernel from the tip. The preferred moisture content is between 60% and 70% on a wet basis (Bagg, 2001).

The most common harvesting systems for whole corn silage use a precision-cut cylinder harvester. This type of machine uses a horizontal drum with several helicoidal knives. The crop is usually cut into lengths varying from 6 to 12 mm. Forage harvesters are manufactured in two configurations: pull-type and self-propelled. In Canada, approximately 475 forage harvesters (pull-type and self-propelled) were sold annually 1991 to 2001 (Canadian Farm and Industrial Equipment, 2002). The self-propelled

forage harvester (SPFH) is a high-capacity machine, over 200 Mg per hour, more adapted to large farms (harvesting ~2000 ha and more of silage), with power requirements commonly in excess of 375 kilowatts. Pull-type forage harvesters (PTFH) generally range in capacity from 40 to 70 Mg (wet basis) per hour and are adapted for smaller farms. The same machines are used to harvest grass, legume and/or whole plant corn silage.

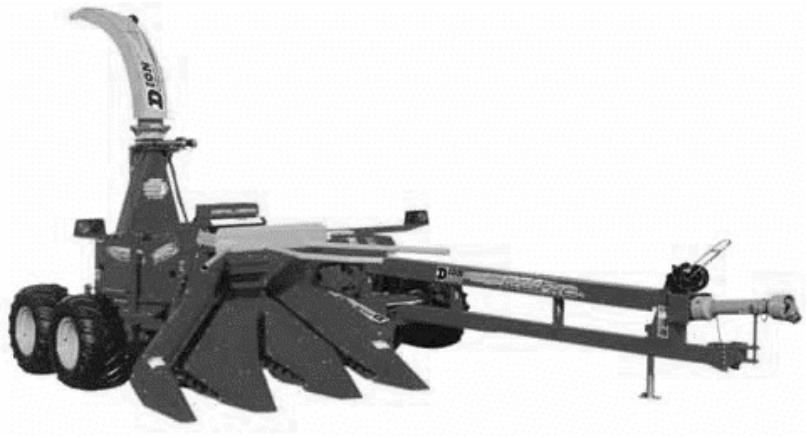

Figure 1.1: Precision cut pull-type forage harvester, with conventional three-row corn header

Different accessories or headers that attach to the harvester exist to either pick up windrows or harvest standing row-crops. Headers are simply switched between crops. Row crop headers are mostly designed for corn harvesting because it is the most common standing silage crop. Grass and legume silage is usually made with wilted grass that has been cut and gathered in windrows 24 to 48 hours earlier. The conventional corn cropping system uses 76cm (30in.) row spacing with a seed population of about 75 000 to 85 000 seeds per hectare. Therefore, the traditional corn headers are designed for this specific spacing. However, new cropping systems have become more popular during the past decade with row spacing of 38, 50 or 106 cm, therefore requiring the development of new corn headers.

Non-row sensitive (NRS) headers have been brought to the North American market only recently and are now commercialized by most manufacturers of self-propelled forage harvesters. This type of headers can harvest a row crop at any row spacing but can also harvest across the rows much more efficiently than traditional headers. This additional

capability can be very useful when harvesting crop perpendicular to the rows, in field corners and other irregular areas. Presently, however, this type of equipment is only available for self-propelled harvesters. In order to develop NRS headers for pull-type harvesters, a study of the power requirements under different conditions is required. By studying and modeling the operation and power requirements, it will be possible to define a basis for design loads and an optimal configuration of a NRS header for a PTFH.

2. LITERATURE REVIEW/BACKGROUND

2.1 Row crop silage harvesting

Most traditional row crop headers are based on the same principle. Rows are divided by gathering points and flare sheets sized to fit the row spacing. Interlocking conveying chains grab the standing stalks, which are then cut by a knife at their base. Knife type varies from manufacturers, but is more commonly a dual cutting disk or sickle bar. The conveying chains then feed the cut plants to the harvester feedrolls.

The main function of the header is to feed the crop to the harvester feedrolls. To do so, row crop headers execute three operations:

- stalk cutting or mowing (row crops are harvested while standing),
- gathering (cut plant material converges to a conveying system) and
- conveying (forage is fed to the feedrolls).

In some cases, gathering and conveying are done simultaneously by the same components such as conveying chains in traditional headers.

2.2 Cutting

Most commercial NRS corn headers use a large serrated disk to cut the crop stalk. In most cases, this operation is done without any countershear device. This type of operation, by which a standing plant is cut using only the inertia and bending resistance of the stalk as a support, is called *free cutting* or *impact cutting*.

The force required to cut a stalk is usually greater than its bending resistance, therefore the inertial forces must provide the complementary resistance. This implies that a

minimum or critical velocity of the knife exists to perform the cut. Different models can be found in literature to estimate this velocity (Sitkei, 1986; Bosoi et al., 1991; Persson, 1987). Those approaches modeled the plant as a cantilever beam under impact loading which caused bending stresses and axial tension in the bottom section of the stalk, due to stalk deflection and constant knife height. The inertia provided a resistance equal to $m_{eq}a$, where m_{eq} is the equivalent mass of the stalk accelerated to knife speed during the cutting and a its acceleration.

Although a theoretical equation for the critical speed can be developed, the difficulty of estimating the equivalent mass analytically makes it seldom applicable. However, Sitkei (1986) described an experimental relationship for the acceleration of the stalk as a function of physical characteristics (EI, where E and I are the modulus of elasticity and cross-section area moment of inertia, respectively) and deflecting strength. This relationship is expressed graphically in literature for only a few values of plant characteristics: m_l, the average mass per unit length of the plant and the physical properties (EI), but no mathematical expression is given. A regression analysis of the graphical data from literature was performed to obtain the following empirical equation for the stalk acceleration:

$$a = \frac{(10.0)(F_c)(EI)^{-0.146}}{m_l}. \tag{2.1}$$

By equating the deflecting strength of the stalk, F_s, to the cutting force, F_c,

$$F_c = F_s = m_{eq} a, \tag{2.2}$$

which defines the conditions of the critical velocity, the equivalent mass, given by F_c/a, can be determined. From dimensional analysis, the acceleration can be used to compute the critical velocity v_{cr} as (Sitkei, 1986):

$$v_{cr} = C\sqrt{d\,F_c/m_l} = C\sqrt{da}, \tag{2.3}$$

where

d : stalk diameter at the cut section (m) and

C: constant ranging from 1 to 1.4**.**

Using typical values of EI, m_l and d from literature (Persson, 1987), the critical velocity to cut a mature green corn stalk was found to range from 6 to 10 m/s. This compares reasonably with critical cutting velocities of crops similar to corn (sunflower and sorghum), which were found to be approximately 10 m/s for most agricultural cutting devices (Bosoi et al., 1991).

The cutting power of a crop can be estimated on an energy basis (per stalk or unit of field area) or by evaluating the cutting force of a single stalk. Some studies (Johnson and Lamp, 1966; Persson, 1987) suggested that the cutting energy of a single stalk was a function of the square of the diameter with a typical value of 15 J for a 38mm diameter stalk, without specifying the type of knife used. Other authors quoted by Johnson and Lamp (1986) suggested static cutting forces ranging from 215 N to 570 N for 30mm diameter corn stalks. However, the value of F_c varies greatly with the condition of the crop. The factors affecting F_c are mainly knife configuration, speed and sharpness, crop type and density, stalk diameter and moisture content, height-of-cut, and forward velocity of the cutting device. The complex and highly variable effects of those parameters, as observed in literature (Persson, 1987), make an analytical estimation of F_c very difficult to obtain.

Most of the data available in literature for cutting energy are relevant to the cutting process in a forage harvester cutterhead (cylinder, flywheel and flail type). Therefore, an experimental determination of the cutting energy would be necessary to obtain values for the knife configuration used on the prototype corn header.

2.3 Gathering

The gathering operation, or otherwise named convergence, consists of feeding the plant material from the cutting system to the conveying system. In conventional headers, this task is done by the same chain/belt system that is used for conveying because they collect the stalks in line with the standing rows. In some designs, stalks are cut after the plant is grabbed by the chains and in others, prior to chain grabbing, without significant

impact on harvesting efficiency (Shields et al., 1982). In the case of headers that cut the plant prior to grabbing it, support for the stem is provided by the surrounding stems still standing and aided by the inertia of the stalk. With higher harvesting speeds, the aerodynamic resistance of the stalk can also become a component of stalk tipping resistance (Bosoi et al., 1991).

In the case of non-row sensitive headers, the stalks can be cut at any position around the frontal periphery of the gathering drums. From the harvesting point, they are gathered to a converging point between two cylinders. In the case of the prototype header to be studied, conveying chains then grab the plant at that position. As opposed to the conventional header, a chain is not present to hold the stalks during the gathering operation. Rather, finger-like protrusions on the drum transport them along the drum periphery. Shielding and other fixed parts create a path to restrict the movement of the gathered crop.

2.4 Conveying

Three common gathering systems incorporating chains are used in row-crop headers: urethane gathering belts, sinusoidal gatherers and zipper steel chains. Shields et al. (1984) studied the harvesting effectiveness between the three systems. These were shown to work equally well in typical harvesting conditions with standing and lodged corn stalks. The power requirements, also, were not significantly different (Shields et al., 1982). The gripping force varied greatly, but it was found that very little stalk crushing was necessary for effective gathering (Shields et al., 1984). Increased crushing could create increased friction in the conveying channel, which, consequently, can boost harvesting power, especially at high throughputs with high stalk density in the gathering chains.

2.5 Header power requirements

Forage harvesting is a high-energy input operation. In addition to cutting the crop in small particles, the forage harvester must gather, compress, convey and blow the crop, from the header to the loading wagon. Most of the energy is used for cutting and blowing the silage, with each accounting for approximately 40% of the total energy. The header and feedrolls account for about 15% of the total power required (O'Dogherty, 1982). This statistic varies with the type of header, the crop harvested, the header design and the cutting cylinder condition (e.g. knife sharpness). In a study, power required for a two-row conventional header was only 2.9 to 3.3 percent of total harvester power and varied linearly with throughput (Shields et al., 1982). An additional, but often negligible energy input by the tractor is also required in the form of tractive effort to accelerate the crop at the speed of the harvester. No data or study related to this matter was found in literature.

Goering et al. (1993) suggested a model to describe the power requirements of a forage harvester header. This model consisted of a term corresponding to the no-load power and a second term proportional to the throughput,

$$P = C_0 + C_1 Q, \tag{2.4}$$

where

C_0: no-load power = P_0 (kW),

C_1: constant for any given header (kW·h/Mg) and

Q : throughput (Mg/h).

The energy input requirement for forage harvesting is expressed as power per unit of material throughput, and called specific energy. Dry matter or wet matter basis can be used. Therefore, the specific energy is given by:

$$SE = \frac{C_0}{Q} + C_1 . \tag{2.5}$$

The curve obtained from the previous equation with *SE* as a function of *Q* is a hyperbole with a horizontal asymptote at C_1. For an ideal header with $C_0=0$, the specific energy becomes constant, or in other words, the efficiency (defined as units of material throughput per units of energy input, or the inverse of the specific energy) of the machine is constant for the whole range of throughput. In actual cases, the efficiency of the machine is increased therefore the input of energy per units of output of processed material (specific energy) is reduced with higher throughputs.

2.6 Properties of corn stalks

2.6.1 Corn stalk cutting energy

In order to develop analytical models of the power requirements for a corn header, corn stalk properties are required. Those properties include cutting energy, crushing resistance, friction coefficient, etc.

Some of the properties of the plant that affect the cutting energy are size, shear strength, friction coefficient and moisture. Several extensive reviews of the cutting mechanism for general and particular cases can be found in literature, where the effects of different properties are illustrated (Persson, 1987; Johnson and Lamp, 1966). However, for silage corn, the conditions encountered are very similar, as most farmers will harvest the corn at the same stage, maturity and moisture content. In addition, the analytical model can be based simply on the cutting energy per stalk as a function of stalk diameter or cross-sectional area, because all the other parameters are relatively constant. The effect of the knife shape has a noticeable impact on the cutting energy of biological material. Therefore, an experiment to validate the cutting energy of corn stalks should be made in conditions as close as possible to the ones encountered in field situations.

Several experimental apparatuses to measure the cutting energy of forage crops have been described in literature. Chancellor (1958) described an apparatus to measure the cutting energy of different knives. The apparatus was a force-displacement recorder

with vertical linear motion. This apparatus allowed the measurement of force and the calculation of energy for cutting single stalks or bundles. The energy computed by this apparatus included the shearing energy and a friction component, which was minimized, between the knife and material. Other cutting-energy measurement apparatuses included rotating impact blades (Chancellor, 1958) on which accelerometers were used to measure the energy absorbed by the rotor. Other methods such as measuring the torque on a forage mower blade do not isolate the shearing energy, but provide a measurement that includes friction and acceleration of the crop material. Depending on the application, isolating the cutting energy is not necessary, which is the case for the proposed research. In a model, the cutting, acceleration and friction can be combined into one energy value for a general crop condition.

2.6.2 Corn stalk crushing resistance

During the gathering operation of the corn header, the corn stalks are compressed between the gathering chains or belts. The force developed on the chains due to this crushing will increase the friction between the chain and the guiding rails; therefore it will have an impact on the power requirements of the header. Johnson and Lamp (1966) showed the relationship between compressive force and deformation perpendicular to the stalk axis.

Three stages of compression were identified (Figure 2.1):

1. compression of woody ring,
2. destruction of woody ring and
3. compression of pith.

The author stated that for green stalks, the compressive resistance was much greater than for dry stalks and the force-deformation curve was nearly linear in all three stages. This suggests different patterns of failure depending on maturity, especially for the breakage of the woody ring which was more sudden for dryer (more mature) stalks. In the third stage, as high relative deformations were reached, the linearity of the curve changed to

an exponential-like curvature as the voids in the stalks were completely crushed (Figure 2.1).

In the same study, a maximum force of 1.55 kN was observed to compress a stalk by 87% of its diameter, using convex surfaces of dimensions similar to a snapping roll found on combine harvesters, which are similar to the dimensions of the conveying chain on the NRS header. No relationship between stalk diameter (or other stalk property) and crushing force could be found, therefore an investigation of these parameters would be useful for the validation of header-specific-energy models.

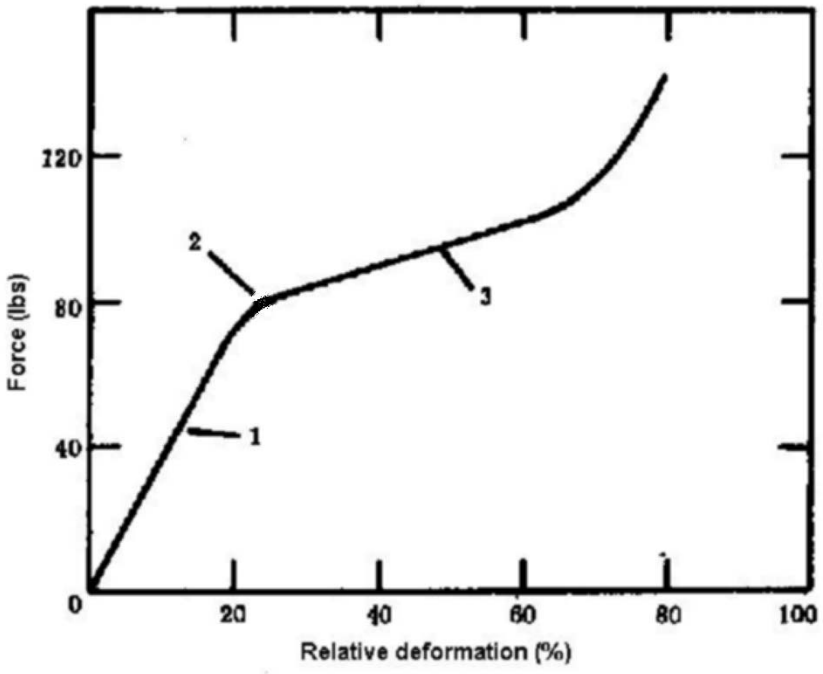

Figure 2.1: Crushing resistance for a dry corn stalk. 1- Compression of woody ring, 2- Destruction of woody ring, 3- Compression of pith. (Adapted from Johnson and Lamp, 1966)

Procedures for a standard compression test of convex-shape food material are listed in the ASAE Standards S368.3 (ASAE, 1999). Equations for the calculation of modulus of elasticity are given for specimens of known Poisson's ratio and radii of curvature. These are based on Hertz equations of contact stresses. They assume very small

deformation and elastic material. Those assumptions do not apply to the scale of deformation encountered during corn harvesting, which often exceed 10 to 20%. Instead, a range of force-deformation values would be more practical.

2.6.3 Corn stalk bending

As previously explained, the critical velocity for cutting depends on structural properties of the plant stem, specifically the modulus of elasticity, *E*. Because corn stalks are not isotropic materials, the modulus of elasticity will change depending on the orientation of stress. A value for *E* can be found for typical loading such as axial tension, radial compression (crushing) and bending. A simple procedure to calculate the modulus of elasticity is to load a corn stalk as a horizontal simply supported beam with a point load at its centre (Figure 2.2). Using a force-displacement apparatus, the deflection and load can be measured.

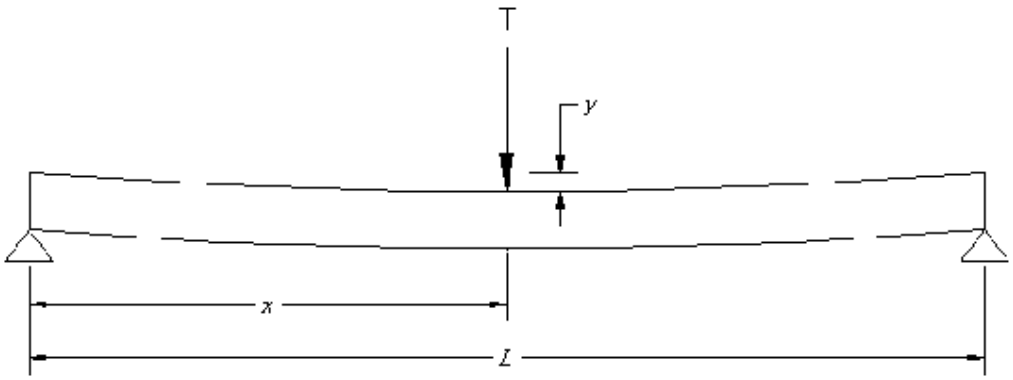

Figure 2.2: Bending of a simply supported beam.

Under the assumptions of the corn stalk being an elastic material and having equal tension and compression moduli of elasticity, the elastic equation (deflection at any point) for a simply supported beam with centred point load is given by:

$$y(x) = \frac{Tx}{12EI}\left(\frac{3}{4}L^2 - x^2\right), \tag{2.5}$$

where

y = vertical deflection of the beam (m),

L = length of the beam (m),

x = position along the beam (m) and

T = point load on beam (N).

The deflection (y_c) at the centre point ($x=L/2$) is then:

$$y_c = \frac{TL^3}{48EI} \tag{2.6}$$

Collecting data on the stalk diameter, d, to obtain the moment of area, I, and recording the load, T, and deflection, y_c, it is then possible to obtain the modulus of elasticity in bending:

$$E = \frac{TL^3}{48Iy_c} \tag{2.7}$$

Johnson and Lamp (1966) described a similar experiment. However, no values of modulus of elasticity are mentioned, but only bending force and deflection at failure. Although all the variables for equation 2.7 are available from this study, they are listed at failure, which is more probably in the plastic region, and are not adequate for modulus of elasticity calculation. From the same study, green stalks (59.8% moisture content) were found to support a greater bending load, but with greater deflection than dry stalks (13% moisture content) (Johnson and Lamp, 1966). Therefore maturity has an effect on the modulus of elasticity of corn stalks.

2.7 Research focus

In summary, no specific documentation on the operation or power requirements of non-row sensitive headers could be found in literature. Several studies presented data specific to the forage harvester cutterhead and blower, but very few on corn headers. Most focused on the harvesting efficiency of traditional headers, in terms of how well they harvest in the field, but no detailed analysis of their power requirements was found. The specificity of each machine and the design of their components, such as the cutting device, made difficult the direct application of data from other research. In order to analyze and model the operation of a non-row sensitive header, specific data related to the header configuration needed to be collected as well as data on crop properties not available in descriptive format in literature, such as crushing resistance.

3. OBJECTIVES

The focus of this research was to observe the operation of a non-row sensitive corn header developed for a pull-type forage harvester in order to better understand its behaviour and power requirements. The results of the analysis and the knowledge gained could then be used to elaborate recommendations to improve the concept and the design of the machine. The general objectives of this study were thus:

- to measure the power requirements of a non-row sensitive corn header and compare them with those of a conventional header,
- to model the header and predict the specific energy requirements in different conditions,
- to validate the model using available literature data complemented with experimental and laboratory data and
- to suggest improvements and modifications on the design with respect to the research performed.

4. EXPERIMENTS

The study of the NRS header consisted of the development of specific energy models and the development of experiments to obtain validation data. Two general sets of experiments were performed. The first set consisted of monitoring and collecting data during the operation of a forage harvester. The second step was directed towards measuring some properties of corn plants such as required cutting energy and crushing resistance.

4.1 Experimental objectives

The purpose of the experiments was to collect data to quantify the parameters involved in the operation of the non-row sensitive header and corn harvesting generally. Power requirements are critical in the design of a machine, as they will dictate the size of components and the constraints that apply to them. In terms of specific energy or energy input per unit of the machine output, in this case the throughput of corn silage, lower values are always pursued because they imply a better energy efficiency of the machine.

The objectives of the experiments were, therefore:

- to measure the specific energy requirements of a NRS header in controlled field conditions,
- to measure the cutting energy of corn stalks with a NRS header cutting blade,
- and to measure the crushing resistance of corn stalks.

4.2 Specific energy measurement

4.2.1 Introduction

The development of a model of specific energy for the headers required experimental data for the calibration and the validation. Field experiments permitted the observation of the particularities of operation of the NRS header compared to the conventional system. The details of the planning and the results of those experiments are provided in this section.

4.2.2 Objectives

The general objective of these experiments was to collect experimental data on the specific energy requirement of a non-row sensitive header for a pull-type forage harvester.

The specific objectives were:

- to operate a non-row sensitive header forage harvester with a pull-type forage harvester,
- to compare the power requirements of that header with those of a conventional 3-row (0.76 m spacing) header,
- to calculate specific energy requirements under different throughput levels,
- to determine the factors affecting the specific energy requirements, and
- to evaluate the effect of the header on the forage harvester operation by measuring the blower power.

4.2.3 Material and Methods

For the first set of experiments, corn silage was harvested with a pull-type precision-cut forage harvester, *Dion* 1224 (Figure 4.1), equipped with a prototype 2.21m non-row sensitive direct cut header (NRS) (Figure 4.3), and a control header, which was a conventional 3-row header (3-R) (Figure 4.4).

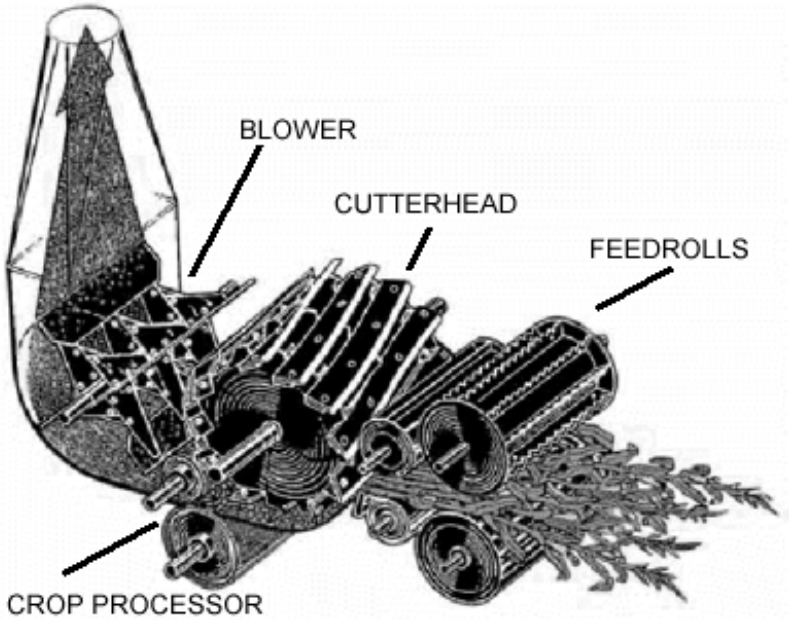

Figure 4.1: In-line configuration of the Dion 1224 forage harvester

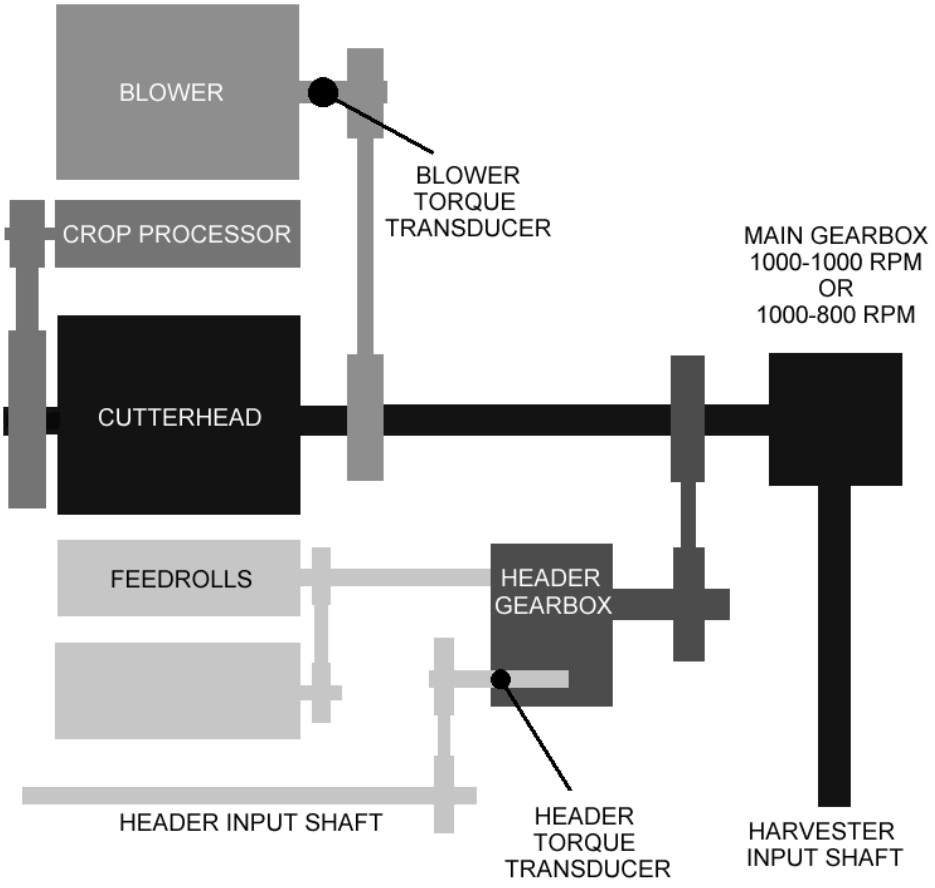

Figure 4.2: Layout of instrumented forage harvester

The forage harvester had a unidirectional configuration, with feedrolls, cutterhead, crop processor and blower all aligned on a single vertical central plane. The harvester was identical to commercial models except for minor modifications required for the instrumentation. Torque transducers were installed to measure torque at the header and the blower. For the header, strain gauge rosettes were installed at the output shaft of the gearbox controlling the operation (forward-neutral-reverse) of the header. The second set of strain gauges were installed directly on the blower shaft (Figure 4.2). The transducers were a pair of two-90-degrees rosettes wrapped around the circumference of the shaft and mounted in Wheatstone bridge arrangement for temperature compensation.

Figure 4.3: Non-row sensitive corn header mounted on a pull-type forage harvester.

The tested prototype NRS header consisted mainly of two drums rotating in opposite directions about vertical axes. The drums were powered by a chain drive, which was also used to convey the stalks gathered between the drums, to the harvester feedrolls module. Disk cutters of 1.05 m diameter were rotating in the same direction as the drums. These disks rotated at a peripheral speed of 14.2 or 17.8 m/s, depending on gearbox settings. Modifications on the frame of the header were required to allow the header to function with the harvester linkage points and lifting ramps. These modifications had no effect on the performance of the header.

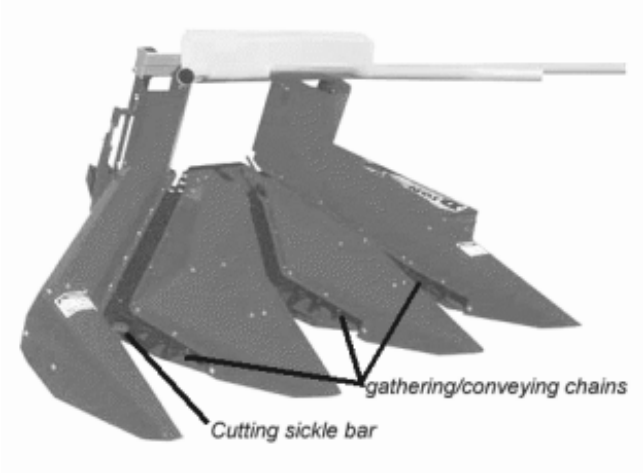

Figure 4.4: Conventional three-row corn header

4.2.3.1 Experiment #1

The harvester was used along with an AGCO 9745 tractor (nominal PTO power of 108 kW and 116kW as tested on dynamometer in summer 2001). The response measured was the strain at the header gearbox output shaft and the blower, measured by means of strain gauges connected to a data logging system. These were converted to torque after calibration and further to power by assuming a constant tractor power take-off (PTO) speed of 1000 rpm therefore assuming a constant header input speed. Calibration curves were established for each strain gauge prior to and after each field test. A slip ring provided continuous gauge signal from the gearbox shaft and data were recorded at a sampling rate of 100 Hz. The factorial experimental design had three treatment factors: the type of header (3-R, NRS), the harvester input speed (154 and 123 rpm) and the forward speed of the tractor (4.5, 5.1, 5.7, and 6.2 km/h). The harvester input speeds were obtained through different main gearboxes with 1:1 (1000 rpm direct drive) or 0.8:1 ratios (1000 rpm PTO to 800 rpm main drive speed reduction). The forward speed provided different levels of throughputs. All treatments were replicated three times during the same day.

The harvesting was done on September 29th 2001 in St-Lin, Québec, Canada. This region records 2600 corn heat units on a typical year. The corn field harvested was organically grown with very uniform characteristics of height (2.5 m approx.), maturity

(2/3 milk line), moisture content and yield. The experimental units were 150 m long field strips of three rows. Silage yields were obtained by weighing the silage boxes with individual scales under each wheel. The weight was then obtained by subtracting the empty weight of the forage box from its full weight. Samples were taken during unloading at the silo and moisture content was calculated according to ASAE Standard 358.2 (ASAE, 1999).

4.2.3.2 Experiment #2

The second experimental site was St-Paul-de-Joliette, Québec, which is in the same area as the site of Experiment #1. The same 1224XC forage harvester and headers (NRS and 3-R) were used along with a John Deere 8410 tractor (nominal PTO power of 175 kW - 191 kW measured on dynamometer in summer 2001). The forward speeds of the tractor were 3.6, 4.6, 5.5, 6.3, 7.1 and 8.0 km/h. Only the 1000 – 1000 rpm gearbox setting was tested at this site. The harvesting was done on October 4th 2001. Soil texture was sandy and the crop had suffered from the drought as practically no cobs had developed. Corn plants height ranged from 1.8 m to 2.1 m. The crop was harvested three rows at a time (0.76 m spacing) on lengths ranging from 80 to 130 meters for each replicate. All treatments were replicated three times on the same day. A commercial freight truck scale was used to weigh the silage boxes with an accuracy of ±10kg. Torque calibration curves and silage yields were obtained similarly as in Experiment #1.

4.2.3.3 Data formatting and filtering

Data were recorded in the form of one-minute files containing 6000 points for both header and blower. A *Microsoft Excel*® macro was written to convert the strain gauge readings to values of power. Noise in the data was removed using the median method, which consisted of replacing each data point by the median of the triplet formed with the previous and following data point. A summary file of all the data obtained by the macro including average header and blower power as well as standard deviations for each of the experimental units was also generated. The standard deviation of each file was used as a measure of the variability of the power demand for the analysis.

4.2.4 Results

4.2.4.1 Raw data

For each test, a plot of the blower and header power with respect to time was created to identify and analyze potential patterns. Figure 4.5 shows a four-second sample of data for the 3-R header and figure 4.6 for the NRS under same levels of treatment (1000-1000 gearbox, 8.0 km/h). Each graph contains 400 data points. It can be seen that both headers required, as expected, much less power than the blower.

The pattern of the data varies greatly between the NRS and the 3-R header. The 3-R header showed high-frequency fluctuations of about 17.5 Hertz while the NRS header curve seemed to follow oscillations of frequency of ~1.1 Hz. An unsuccessful attempt was made to relate those frequencies with the speed of internal components of the headers. For the (3-R) header, the fastest moving component was the sickle bar mower which rotated at a speed of 630 rpm or 10.5 Hz. No explanation for the 17.5 Hz load frequency could be found. From the visual observations of the machine in operation, the irregular but cyclical power demand curve of the NRS header was probably due to the formation of clumps of stalks in the gathering portion of the harvesting action. As the clumps were formed and conveyed to the feedrolls, they created power peaks.

The power delivered to the blower unit also varied with a relatively constant frequency. For both headers, the frequencies were similar with a value of ~7.4 Hz for the 1000-1000 gearbox and ~6.1 Hz for the 1000-800 gearbox respectively. One can assume those power oscillations were due to varying loads coming on the impeller blades, propelling the silage in the spout at regular intervals. Considering that the blower rotated at speeds of 1750 rpm (1000-1000) and 1440 rpm (1000-800) and had four blades, theoretical load frequencies of 117 Hz and 96 Hz should result. Because the data logger was recording at a rate of 100 Hz, the theoretical frequencies could not have been measured since the maximum frequency measurable corresponds to half the sampling frequency, called *Nyquist frequency*, in this case, 50 Hz. The relatively low load frequencies were probably due to aliasing, the phenomenon by which a false low frequency is observed from the analog-to-digital transformation of a high frequency

signal (Figliola et al., 2000). The shape of the signal and the amplitude of the wave observed are not always accurate, but the average can be used if done over a large number of cycles, which was the case for these tests where the average was done over several hundreds of cycles of the alias.

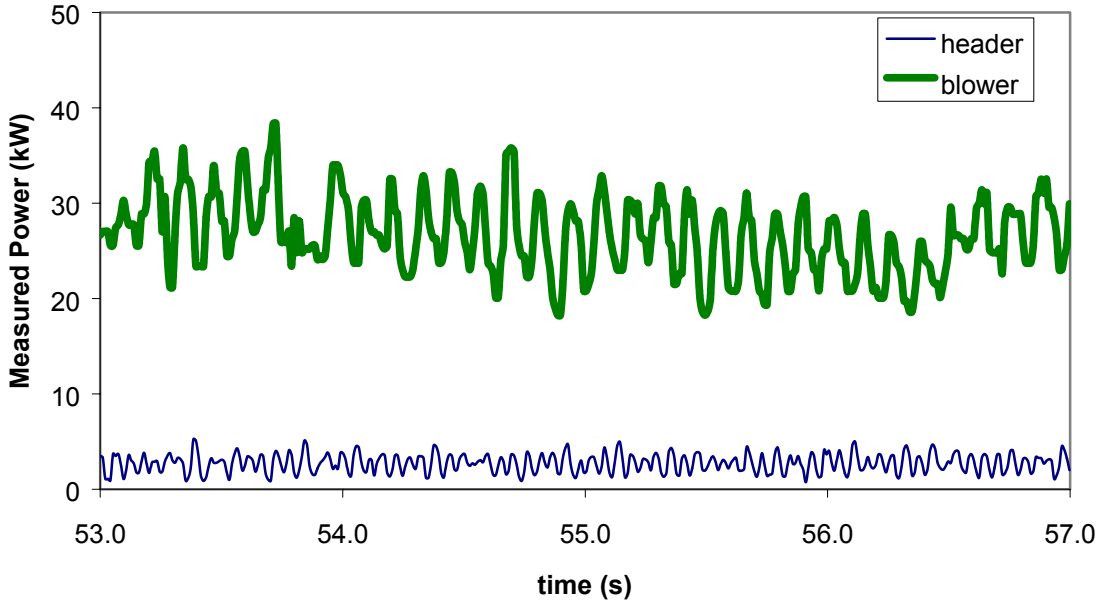

Figure 4.5: Data sample of power measured with 3-R header

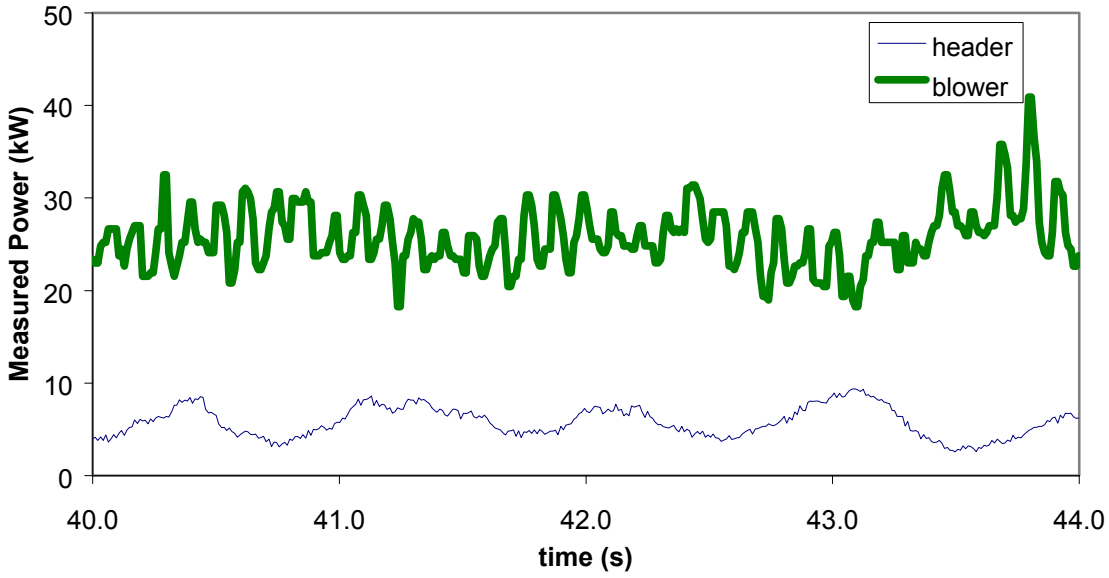

Figure 4.6: Sample data of power measured with NRS header

A further analysis of the variability of the power demand was done by inspecting and comparing the coefficient of variation (CV) of the one-minute data files. Figures 4.7 and 4.7 are plots of the power coefficients of variation with respect to the average power at the header and blower, respectively. For the headers, the average CVs were 0.411 and 0.397 for NRS and 3-R headers, respectively, and these were not statistically different at 5% significance level (p=0.20). However, they seemed to follow a decreasing trend with increasing average power. This means that at higher throughputs, the variability of the power reduces. This is probably due to the more constant flow of material through the header as the rate of plants harvested increased. Each plant harvested can be seen as a discrete event causing power demand fluctuations for finite periods of time.

In the case of the blower power CVs, no significant trend was detected and the averages for the NRS and 3-R header treatments were 0.235 and 0.240, respectively, and these were not statistically different at the 5% significance level (p=0.55).

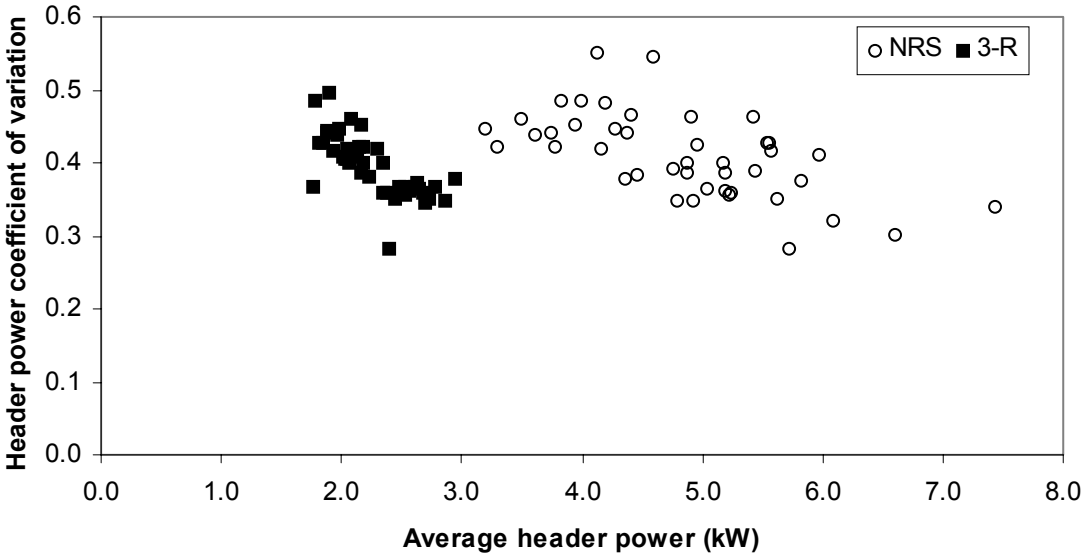

Figure 4.7: Coefficient of variation of header power (All tests)

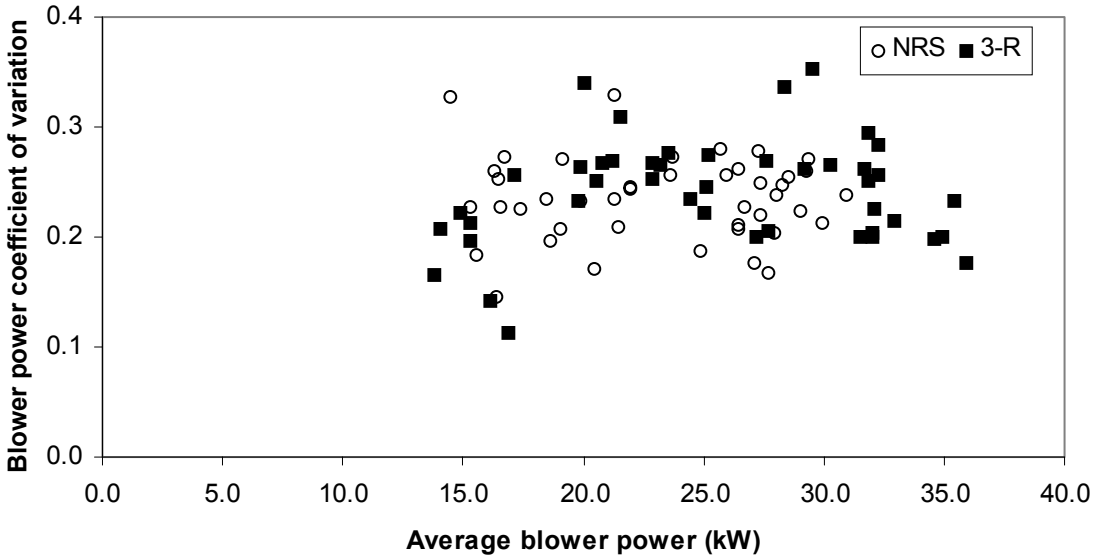

Figure 4.8: Coefficient of variation of blower power (All tests)

4.2.4.2 Specific energy

Tables 4.1, 4.2 and 4.3 show the detailed results of zero-throughput power and the specific energies calculated for experiments 1 and 2, respectively.

Table 4.1: Zero-throughput power requirements for a non-row-sensitive (NRS) and three-row (3-R) crop header.

Gearbox	Header Type	Power (kW)
1000-800	NRS	2.3
1000-1000	NRS	2.7
1000-800	3-R	1.2
1000-1000	3-R	1.4

Table 4.2: Power requirements for non-row-sensitive (NRS) and three-row (3-R) crop headers to harvest corn silage with a pull-type forage harvester in experiment #1 (n=3).

Gearbox	Header type	Forward speed (km/h)	Yield (Mg/ha)	Moisture content (%)	Throughput (t DM/h)	Average header power (kW)	Peak header power (kW)	Average header SE[+] (kW·h/Mg DM)	Standard deviation of header SE 3 rep. (kW·h/Mg DM)	Average blower power (kW)	Peak blower power (kW)	Average blower SE (kW.h/Mg DM)	Standard deviation of blower SE (kW·h/Mg DM)
1000-800	NRS	4.5*	35.1	62.7	13.4	4.18	7.31	0.31	0.060	21.6	35.1	1.61	0.170
		5.1	35.1	62.7	15.2	4.15	7.31	0.27	0.060	21.7	34.1	1.43	0.321
		5.7	35.1	62.6	17.0	4.42	7.88	0.26	0.034	24.5	36.9	1.44	0.238
		6.2	35.1	62.6	18.5	5.08	8.76	0.27	0.052	28.5	43.3	1.54	0.025
1000-800	3-R	4.5	35.1	64.1	12.9	1.98	4.54	0.15	0.009	25.9	39.9	2.00	0.459
		5.1	35.1	64.1	14.6	1.91	4.43	0.13	0.012	25.8	38.8	1.76	0.433
		5.7*	35.1	63.9	16.4	1.99	5.03	0.12	0.008	27.6	40.8	1.68	0.380
		6.2	35.1	63.5	18.1	2.19	5.10	0.12	0.006	34.3	48.6	1.90	0.116
1000-1000	NRS	4.5	35.1	63.9	13.0	5.17	9.32	0.40	0.034	25.5	42.3	1.96	0.258
		5.1	35.1	64.6	14.4	5.12	9.17	0.36	0.081	27.1	44.2	1.88	0.161
		5.7	35.1	64.2	16.3	4.84	9.22	0.30	0.076	29.5	46.9	1.81	0.213
		6.2	35.1	64.6	17.6	5.33	9.63	0.30	0.050	27.7	43.3	1.58	0.155
1000-1000	3-R	4.5	35.1	63.8	13.0	1.93	4.06	0.15	0.007	24.8	40.9	1.90	0.204
		5.1	35.1	63.8	14.8	2.02	4.34	0.14	0.005	30.6	48.7	2.08	0.154
		5.7	35.1	63.8	16.5	2.11	4.48	0.13	0.007	33.1	50.5	2.01	0.120
		6.2	35.1	64.1	17.8	2.13	4.68	0.12	0.004	31.3	46.5	1.76	0.035

[+] SE = Specific Energy

* Two replicates only

Table 4.3: Power requirements for non-row-sensitive (NRS) and three-row (3-R) crop headers to harvest corn silage with a pull-type forage harvester in experiment #2 (n=3).

Gearbox	Header type	Forward speed (km/h)	Yield (Mg/ha)	Moisture content (%)	Throughput (t DM/h)	Average header power (kW)	Maximum header power (kW)	Average header SE [+] (kW.h/Mg DM)	Standard deviation of header SE (kW·h/Mg DM)	Average blower power (kW)	Maximum blower power (kW)	Average blower SE (kW·h/Mg DM)	Standard deviation of blower SE (kW·h/Mg DM)
1000-1000	NRS	3.6	18.6	70.4	4.6	3.47	6.43	0.76	0.100	15.5	30.3	3.37	0.376
		4.6*	18.6	70.4	5.8	4.59	7.14	0.79	0.113	16.4	28.0	3.86	0.074
		5.5	19.9	69.8	7.7	4.33	7.78	0.57	0.048	18.8	27.8	2.48	0.494
		6.3	19.9	69.8	8.7	4.84	8.46	0.56	0.049	22.1	32.5	2.60	0.443
		7.1	19.9	69.8	9.9	4.86	8.33	0.50	0.074	20.9	28.5	2.15	0.578
		8.0	19.9	69.8	11.3	5.31	8.82	0.47	0.052	27.4	36.0	2.45	0.289
1000-1000	3-R	3.6*	22.3	69.1	5.7	2.43	4.45	0.43	0.032	14.7	22.0	2.58	0.129
		4.6	22.2	69.6	7.1	2.45	4.46	0.34	0.011	17.0	25.6	2.37	0.420
		5.5	22.3	69.6	8.4	2.47	4.50	0.29	0.024	19.0	26.8	2.27	0.459
		6.3	22.3	69.6	9.7	2.71	5.09	0.28	0.019	26.8	39.1	2.76	0.786
		7.1	22.2	70.0	10.6	2.69	4.91	0.25	0.018	25.3	36.8	2.40	0.446
		8.0	22.2	69.6	12.3	2.72	4.97	0.22	0.004	26.6	36.3	2.15	0.229

[+] SE = Specific Energy
*Two replicates only.

The measured yield, forward speed and moisture content were used to calculate the throughput in order to compute the specific energy required by the header or the blower. Tables 4.2 and 4.3 give averages of three test replications. Two tests in each experiment were only replicated twice since some replications had to be discarded due to severe noise distortion or data loss.

A first look at the results shows that, for the NRS header, power requirements were more than twice as large as for the 3-R header in both experiments. The same observation can be made with respect to the zero-throughput power or minimum power. The NRS header contained more moving parts and frictional components than the 3-R one. The power required by the blower was very similar for both machines and approximately 10 to 15 times higher than the 3-R header power and 5 to 7 times for the

NRS header. The average specific energy at the header and the blower are shown graphically in figures 4.9 and 4.10.

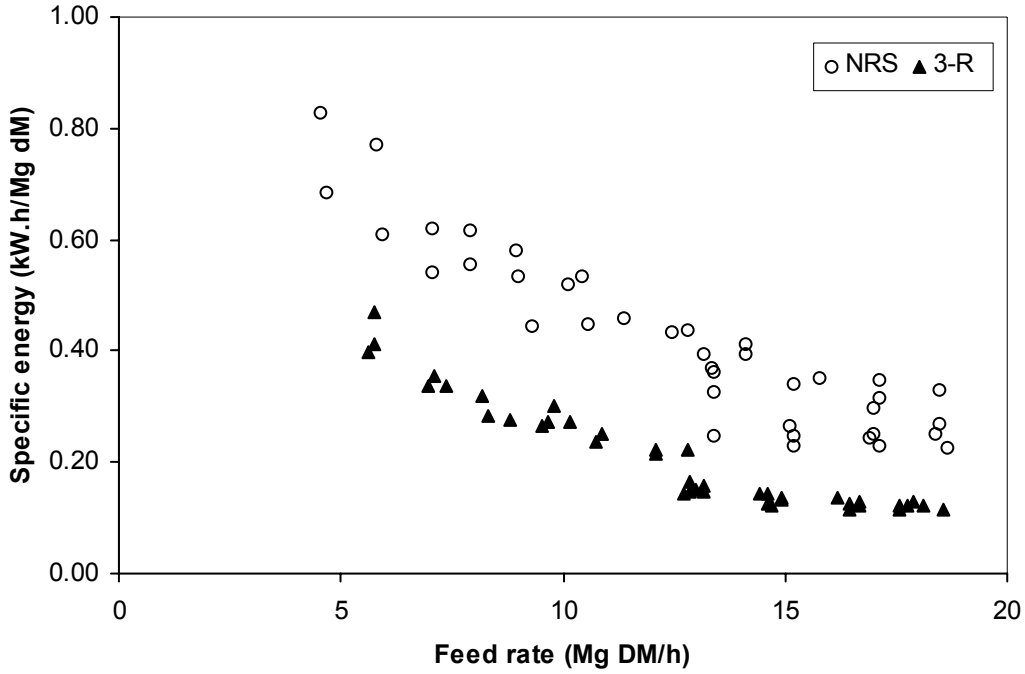

Figure 4.9: Average header specific energy (all tests)

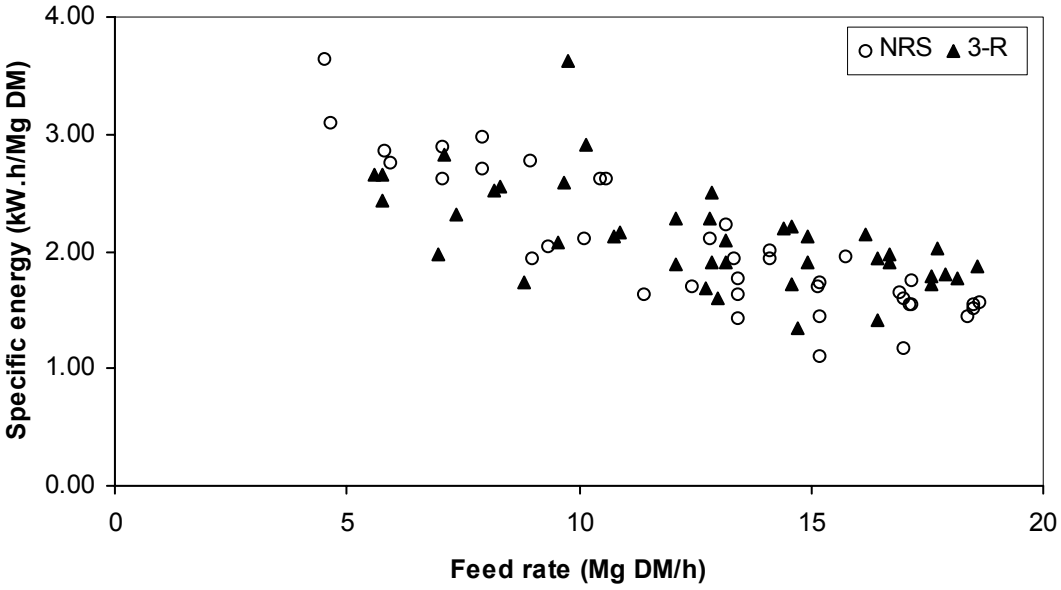

Figure 4.10: Average blower specific energy (all tests)

Ratios of maximum to average power were also calculated. The NRS header mean ratio was 1.76 and 2.05 for the 3-R header, which were statistically different at the 5% significance level ($p<0.01$). At the blower, the ratios were 1.56 and 1.48 for the NRS and 3-R header respectively. They were also statistically different at the 5% significance level ($p<0.01$). The large inertia of the components of the NRS header probably explains the lower maxima, while the more fluctuating flow of crop with the NRS explains the higher ratio at the blower.

4.2.4.3 Statistical analysis

A statistical analysis of the data was used to determine the significance of the effect of different operating parameters on the specific energy requirement of both headers. Analyses of variance (ANOVA) were performed using *SAS* general linear model procedure to test the significance of the three fixed effects in the experiments: header type, gearbox configuration and forward speed. This analysis was done on the header average (AVGHSE) and peak (MAXHSE) specific energy and on the blower average (AVGBSE) and maximum (MAXBSE) specific energy values.

In experiment #1, all three factors were tested giving the following model for the ANOVA,

$$SE_{ijkl} = \mu + h_i + g_j + s_k + (h_i * g_j) + (h_i * s_k) + (g_j * s_k) + (h_i * g_j * s_k) + e_{ijkl}, \qquad (4.1)$$

where

μ: overall average,
h: header treatment effect,
g: gearbox treatment effect,
s: forward speed treatment effect,
$h*g$: interaction effect between header and gearbox,
$h*s$: header-transmission interaction,
$g*s$: gearbox-speed interaction,
$h*g*s$: header-gearbox-speed interaction,
e : experimental error,

and

i = 1, 2 refers to the header,
j = 1, 2 the gearbox used,
k = 1- 4 the forward speed and
l = 1- 3 the replicates.

The details of the analysis are shown in Appendix 1. It was observed that the header, gearbox and forward speed had statistically significant effect on the average header specific energy demand (Table 4.4), as well as the interaction between gearbox and header. No least significant difference was calculated for the means of speed treatments due to unequal replicates for causes listed previously. The header type had an effect on the four responses evaluated.

The blower specific energy requirements were only affected significantly by the header and gearbox. The gearbox effect was expected partly because of the non-linear relationship between fan speed and air resistance.

Table 4.4: Statistically significant treatment effects at 5% significance level by ANOVA (Experiment #1).

Factor	Average header specific energy	Maximum header specific energy	Average blower specific energy	Maximum blower specific energy
Header	X	X	X	X
Gearbox	X		X	
Speed	X			
Header*Gearbox	X	X		
Header*Speed				
Gearbox*Speed				
Header*Gearbox*Speed				

X: significant effect at 5% significance level.

In experiment #2, only the header and speed factors were tested. Therefore, the linear model for the ANOVA with the two fixed factors was:

$$SE_{ikl} = \mu + h_i + s_k + h_i * s_k + e_{ikl} \quad . \tag{4.2}$$

Table 4.5 summarizes the details of the analysis listed in Appendix 2. Inconsistent results were obtained when comparing experiments #1 and #2. Speed had significant effect on MAXHSE in experiment #2 but not in #1, while header effect was significant on the AVGBSE in experiment #1, but not in #2. Conclusions on maximum specific

energy should be carefully interpreted, because they represent maxima that can be cause by field variations, operator actions or other causes not necessarily related to the design of the header. The large no-load power of the blower and the relatively small values of throughputs tested in experiment #2 may explain the undetected header effect on AVGBSE.

Table 4.5: Statistically significant treatment effects at 5% significance level by ANOVA (Experiment #2).

Factor	Average header specific energy	Maximum header specific energy	Average blower specific energy	Maximum blower specific energy
Header	X	X		X
Speed	X	X		X
Header*Speed				X

X: significant effect at 5% significance level.

The ANOVAs were done using forward speed as a factor. The velocity of the header main effect was to increase the throughput for a given uniform yield. Therefore, a statistical analysis that uses throughput instead of forward speed as a factor affecting specific energy requirements could be more conclusive. Moreover, the yield was measured in the field for all tests, in small groups of replicates therefore providing a good estimate of the yield for each test instead of assuming an equal average yield over the field. Because for each test, throughput (Q), in units of Mg of dry matter per hour, was an independent quantitative factor, an analysis of covariance (ANCOVA) was appropriate. The throughput Q was calculated using the forward speed and the measured yield in each test section.

The models for the analysis were:

$$SE_{ijl} = \mu + h_i + g_j + h_i * g_j + \beta Q_{ijl} + e_{ijl} \quad (4.3)$$

for experiment #1 and

$$SE_{il} = \mu + h_i + \beta Q_{il} + e_{il} \quad (4.4)$$

for experiment #2,

where β is a regression coefficient on the throughput, Q.

Tables 4.6 and 4.7 summarize the ANCOVA results for experiment #1 and #2. The details of the analysis are listed in Appendices 3 and 4.

Table 4.6: Statistically significant factors at 5% significance level by ANCOVA (Experiment #1).

Treatment	Average header specific energy	Maximum header specific energy	Average blower specific energy	Maximum blower specific energy
Header	X	X	X	X
Gearbox	X		X	
Header*Gearbox	X	X		
Q	X	X		

X: significant effect at 5% significance level.

Table 4.7: Statistically significant factors at 5% significance level by ANCOVA (Experiment #2).

Treatment	Average header specific energy	Maximum header specific energy	Average blower specific energy	Maximum blower specific energy
Header	X	X		
Q	X	X	X	X

X: significant effect at 5% significance level.

4.2.5 Discussion

The measurements done during the experiments provided a large amount of information on the operation of both the NRS and 3-R headers. Not only average specific energies have been calculated, but also patterns of variability have been detected and associated to visual observations of the machine in operation, as in the case of the low frequency power demand curve of the NRS header.

The major difference observed between the two header types was the zero-throughput or base power, which was twice as large for the prototype. The conventional header contained fewer moving parts, mostly sprockets and chains, while the NRS header tested had many, and some large, moving parts such as the harvesting drums. The

multiplication of bearings and frictional components largely explained the divergence in energy requirements.

The analysis of covariance, ANCOVA, when compared to the ANOVA, detected more effects that are significant. As seen in tables 4.6 and 4.7, throughput, header type and gearbox are the effects that must be considered in the modeling of the specific energy requirements. The fact that a gearbox-header interaction was found suggests different functions of the power demand of the two headers with respect to input speed, certainly due to the different designs.

The measurements of the blower specific energy were made in order to determine the existence of potential effects of the header on the energy demand of the rest of the harvester. Irregularities in feeding of the crop could result in higher variability of the blower power demand. The statistical analysis showed conflicting conclusions on that matter with significant effect of the header on the average blower power detected in experiment #1 but not in experiment #2. A more consistent result was obtained when looking at the maximum blower power where significant effects were detected in the majority of the tests. As mentioned, the design of the NRS header was more susceptible to variable feeding because of the absence of conveying chains to hold the crop from the cutting to the delivery to the feedrolls. The comparison of the coefficient of variation of the blower specific energy, however, did not detect this difference at the 5% significance level.

4.2.6 Conclusions on specific energy measurement

The analysis of the field data obtained in this set of experiments and the observation of the working prototype provided the following conclusions:

- A non-row sensitive corn header was operated successfully with a pull-type forage harvester in field conditions. Necessary modifications were made to adapt the prototype to the harvester without affecting its functioning.
- The power and specific energy requirements of the NRS prototype and a conventional three row header were measured and calculated. The average energy required by the NRS header was 0.43 kW.h/Mg, approximately twice as much as the conventional header's 0.21 kW.h/Mg. The conventional header power demand was more variable and varied with a higher frequency than the NRS header.
- By statistical analysis, the main factors affecting the specific energy requirements of the header and blower were found to be the header, the gearbox or input speed, and the throughput. The difference in design, and more specifically the size and the number of moving parts probably explains most of the differences in specific energy requirements of the two tested headers.
- No clear effect of the type of header on the specific energy requirements of the blower was detected except for higher peak-to-average power ratio with the NRS header.

4.2 Cutting energy measurement

4.2.1 Introduction

The development, validation and use of an analytical model of the NRS header required data on the properties of the crop to be harvested or data on the operation of the machine in field conditions such as the cutting energy for a given crop. Appropriate and efficient cutting of the plant is critical to the good operation of a harvesting machine. Many factors affect the required cutting energy of a plant, some relating to the plant itself, others to the cutting device and the interactions between both. The scope of this research was limited to one type of knife, a serrated knife blade as used on the NRS header.

4.2.2 Objectives

In the context of the modeling of the energy requirements of a non-row sensitive header, the objectives of this work were:

- to measure the cutting energy of corn stalks using a non-row sensitive header knife in conditions similar to field conditions,
- to compare the energy requirements for two knife configurations, and
- to develop a relationship between corn stalk dimensions and cutting energy.

4.2.3 Material and methods

4.2.3.1 Apparatus

Two different knife sections from the prototype NRS header were tested, one from a second-generation prototype (knife A) and one from the header prototype used in the specific energy experiment (knife B) (Figure 4.11). Knife (A) consisted of a 60^{o} arc section with a tip radius of 0.712 m and a thickness of 3 mm. Knife (B) was a circular knife quarter section of 4.8 mm thickness with a tip radius (L_k) of 0.555 m. The shape of the teeth was very similar and of same scale of dimension for both knives. The teeth were triangular with the cutting edge positioned 22^{o} forward of the knife radius (in the cutting direction). The angle at the teeth tips was 45^{o}. Only the radius and thickness of

the knives differed. The teeth pitches were 50mm and 48mm for knives A and B, respectively.

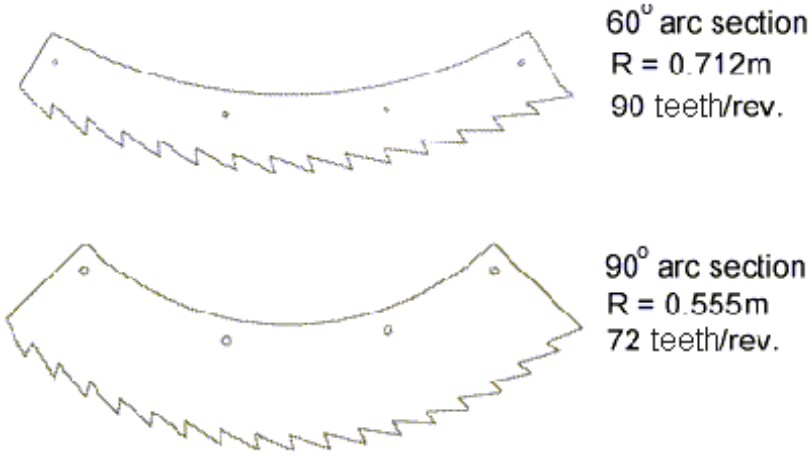

Figure 4.11: Knife blades used in the experiment: Knife-A (top) and knife-B (bottom)

An experimental apparatus was designed and built to measure the cutting energy of the stalks (Figure 4.12). It consisted of a pendulum assembly on which the knife sections were attached. The pendulum was mounted on a tube frame and rotated about a horizontal axis, supported by pillow block ball bearings to allow free oscillation with minimal friction. Square tubing and steel plates were used to build the pendulum. The apparatus was designed using CAD software that allowed the calculation of the mass, m, centre of gravity location, R, and moment of inertia, I_o, of the rotating knife-pendulum assembly (Table 4.8). Those values were necessary to later calculate the cutting energy.

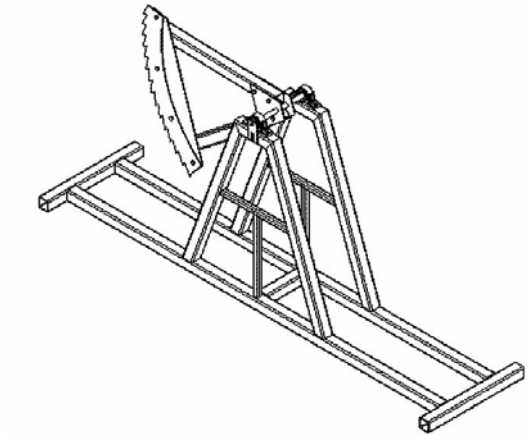

Figure 4.12: Experimental Cutting Energy Measurement Device

Table 4.8: Pendulum physical properties

	Knife A	Knife B	
Mass *(m)*	10.9	10.9	kg
Radius to C.G. *(R)*	0.357	0.276	m
Moment of inertia *(I_o)*	0.829	0.521	$kg.m^2$
Blade radius *(L_k)*	0.712	0.555	m

Two sets of knife supports were designed to match knife A and B. Knife blades were rigidly attached to the supports with bolts, and the support itself was bolted to the pivoting shaft. The knife supports were designed to offset the outside radius at one extremity of the knife to simulate the path of the knife, which would be observed in a field situation with a harvester speed of approximately 5 km/h.

A position sensor was attached to the rotating shaft supporting the knife. A 1-turn 1-kΩ low-friction potentiometer with continuous resolution was used. It was wired to a data logger (CR10X, Campbell Scientific Inc., Logan, UT) with constant 5V excitation voltage provided by the logger. The three pin potentiometer was used as a voltage divider circuit. The excitation voltage was applied to the outer pins across the full length of the resistor. The voltage output (signal) was taken between one outer pin and the middle pin. Therefore, the resistance across the output pins varied as a fraction of the total resistance with respect to the position, giving a linearly proportional output voltage which was recorded by the logger. The position was sampled at the maximum rate, of 64 Hz, offered by the logger. A toggle switch allowed easy control of the sampling.

4.2.3.2 Methodology

Whole corn plants were collected in the fall on a farm in the Saskatoon region. The corn was planted at standard 76cm spacing with a seed population of ~75000 seeds/ha. The field was irrigated during the growing season. The variety used required 2000 corn heat units to reach maturity and was very uniform in appearance and height (~2.15m). The plant specimens were randomly harvested across the field on October 4th 2002, the same day the field was harvested for silage production. The cutting energy experiment was

also done on the same day. The 75 specimens were cut at the surface of the ground and kept outside until the time of the experiment.

Each specimen was identified randomly and the stalk base minor and major diameters were measured 0.15m above the base and recorded. Two groups were made. A first group of 50 specimens was randomly selected for testing using knife A and the 25 others using knife B. More specimens were used for knife *A* to obtain a larger sample size to investigate the correlation between stalk dimensional characteristics, with cutting energy. Extra specimens were used to measure the whole plant and stalk moisture content according to ASAE Standard S358.2 (1999). Whole plant moisture was 68.2% wet basis (w.b.), which corresponded with the recommended range for silage. Stalk moisture content was 80.8% w.b. The experimental design was a completely random design with two treatments (knives A and B).

The stalks were solidly held at their bases on the pendulum frame by a pipe clip to simulate the plant as it is standing in the field. The distance from the base of the stalk to the knife was approximately 0.15m, where the diameter measurements were made, which corresponded with common height of cut in the field. A square tubing section (50 mm side) served as a guide to support the stalk on the other side of the knife at a distance of 10 cm. The stalks were slid into the tube. This simulated the countershear action of the gathering teeth on the prototype header and prevented bending of the stalks due to the horizontal position. The height of the stalk ensured complete cut by the passing of the knife blade.

Before positioning the specimen, the pendulum was rotated up and held in place in a predefined position. When the stalk was in place, the toggle switch was turned on to start the data sampling, and the pendulum was released to cut the stalk. After the first oscillation was completed, the toggle switch was turned off. Each blade was tested in one session to avoid numerous blade changes.

By measuring the starting and end points of the oscillating pendulum, it was possible to calculate the energy absorbed by the knife to cut through the stalk. Setting the datum for potential energy when the pendulum was at rest, the potential energy for any angular position was given by:

$$PE = mgR(1 - \sin\theta), \tag{4.5}$$

where:

m: mass of the pendulum (kg),
g: gravitational acceleration (m/s^2),
R: radial length to centre of gravity (m) and
θ: angular position of the pendulum (radians),

as illustrated in Figure 4.13.

By releasing the pendulum assembly from a given position, the potential energy was transformed into kinetic energy with the rotation of the pendulum. Some energy was dissipated due to friction in the bearings and some was absorbed to cut the corn stalk. This energy absorption resulted in a change in the position at the end of the half-cycle. Therefore, by monitoring the position of the pendulum, it was possible to measure the energy absorbed during the cutting process.

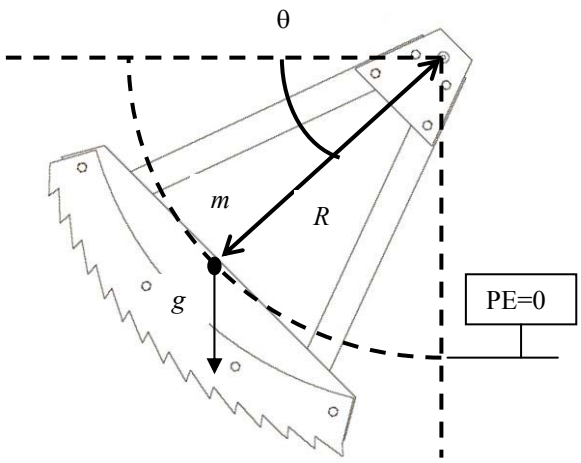

Figure 4.13: Schematic view of the pendulum apparatus

4.2.3.4 Calibration

A calibration was required to transform the voltage data obtained from the potentiometer into an angular value. The pendulum assembly was designed so that the centre of gravity was aligned with the centre of the knife blade. This was confirmed by verifying the vertical alignment of the blade centre with the pendulum shaft when at rest. The whole apparatus was levelled, and then the pendulum was positioned at different angles using a bevel protractor. This calibration was repeated five times throughout the experiment. Voltage output at rest was verified to correspond to 90^{o} as obtained by the linear regression performed on the calibration data (Appendix 5).

Although the apparatus was designed with bearings to reduce friction losses, theses losses were accounted for in the calculation of the cutting energy. The losses came mainly from the friction inside the bearings and air resistance during the oscillation. Six test runs were done for each blade-pendulum starting at two different positions. The friction force is generally proportional to the normal force on the bearing. Therefore, the energy losses might not have been linear with the total displacement of the pendulum, due to the varying centrifugal force exerted by the swinging mass. However, the loss was considered relatively constant and an average value of energy per angle of rotation was calculated and later used to approximate the losses for each test run with stalk cutting (Appendix 5). The potential energy of the pendulum was calculated while in starting position and its final potential energy was determined after a half oscillation, at the maximum height reached. The difference in the two energy levels calculated corresponded to the energy loss. This value was divided by the travel of the pendulum to obtain an average energy loss per unit of angular travel (degree).

4.2.4 Results

Using the data logger, data for position versus time were recorded for each of the 75 cutting tests. The voltage readings were transformed into position and only the first half-cycle was retained. A plot of the data for each pendulum is shown in Figure 4.14 and Figure 4.15 with cutting and without cutting (knife alone). The moment at which the pendulum impacts the stalk is also indicated on the graph. The effect of cutting on

the movement of the blade is clearly noticeable. It is observed that the height reached at the end of the half-cycle is reduced and the apparent period of the pendulum was extended.

Some test results were rejected mostly due to incomplete cutting where the pendulum remained stuck with the stalk. This happened with larger stalks requiring more energy to be cut. The first tests were done with a starting angle of 20^o from the horizontal, which was then changed to 5^o to allow a larger starting energy. Examples of tests with incomplete cut can be seen in Figure 4.14 in which the knife was blocked at the position where it impacted the stalk. The final count of useful specimens was reduced to 39 and 17 for blades A and B, respectively.

The starting and ending angles were compiled in Tables 4.9 and 4.10 along with the stalk dimension. The shape of the stalk cross-section was modeled as an ellipse with minor and major diameters, d and D, respectively. The equivalent diameter, D_{equ}, was calculated as the diameter of a circle with the same area as an ellipse of diameters d and D.

This value is given by:

$$D_{equ} = \sqrt{dD} \quad , \tag{4.6}$$

because the area of an ellipse (m^2) is:

$$A = \frac{\pi}{4} dD \, . \tag{4.7}$$

The cutting energy was calculated by subtracting, from the starting potential energy, the ending potential energy and the frictional energy loss calculated according to the previously determined relationship.

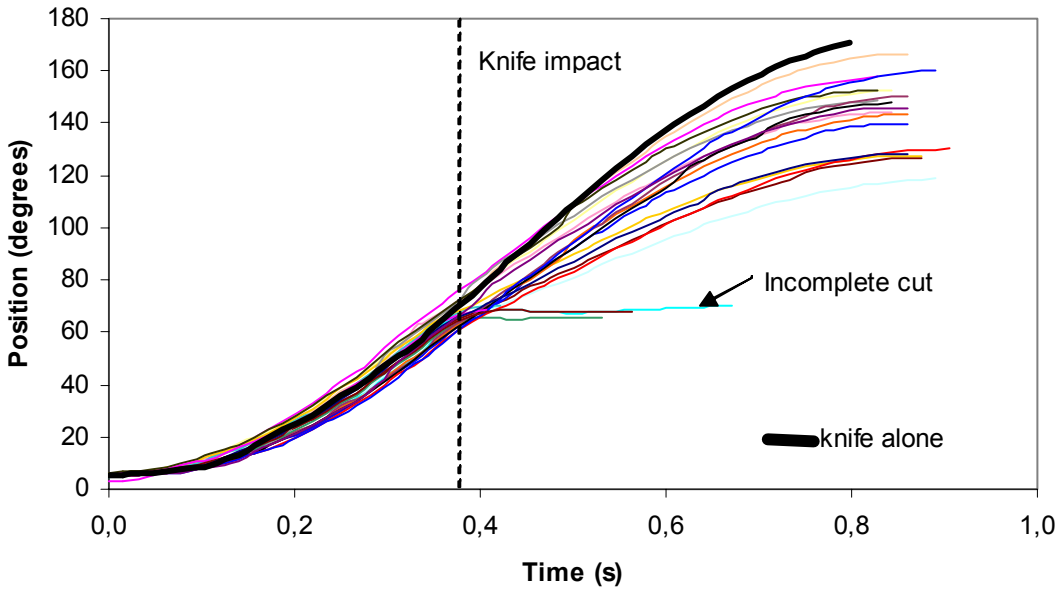

Figure 4.14: Samples of test data for corn stalk cutting with knife-pendulum A

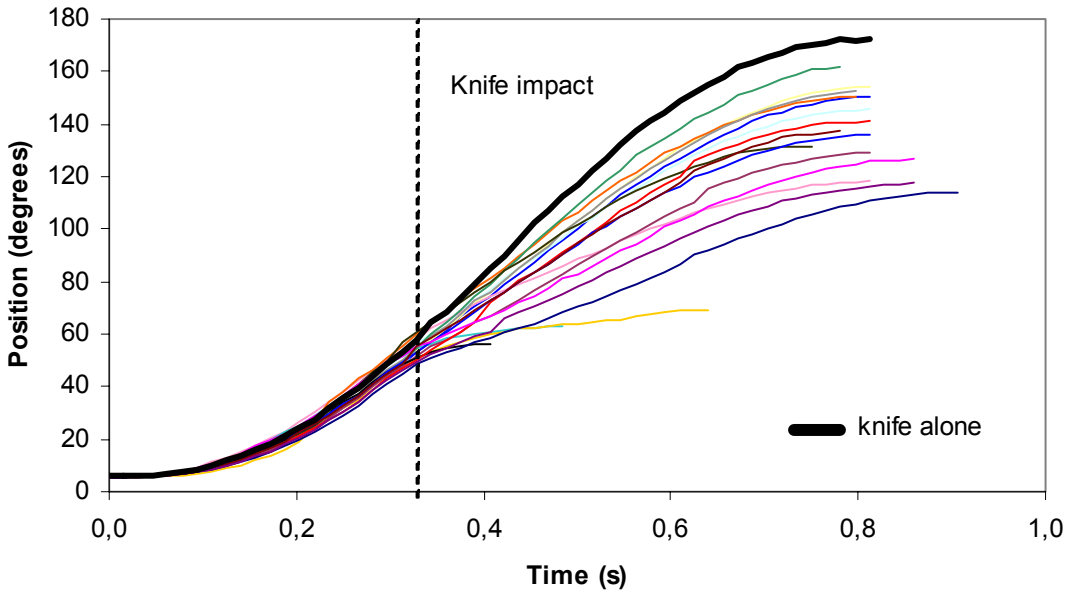

Figure 4.15: Samples of test data for corn stalk cutting with knife-pendulum B

Table 4.9: Cutting energy results for knife-pendulum A

Test #	Minor diameter d	Major diameter D	Equivalent diameter D_{equ}	Cross-section area A	Starting angle θ_{start}	Ending angle θ_{end}	Pendulum starting Energy E_{start}	Pendulum ending energy E_{end}	Energy loss E_{loss}	Cutting energy E_{cut}
	mm	*mm*	*mm*	*mm²*	*deg.*	*deg.*	*J*	*J*	*J*	*J*
A23	25.2	23.8	24.49	471.1	19.8	116.0	13.00	34.38	0.59	20.79
A24	14.9	13.8	14.34	161.5	19.8	133.3	13.00	27.80	0.70	14.11
A25	18.2	15.3	16.69	218.7	19.9	119.8	13.04	33.17	0.61	19.51
A26	23.3	20.6	21.91	377.0	20.4	129.8	13.34	29.35	0.67	15.34
A28	16.1	14.3	15.17	180.8	19.7	132.1	12.91	28.36	0.69	14.76
A30	22.8	20.2	21.46	361.7	20.6	130.2	13.51	29.22	0.67	15.04
A31	20.0	17.2	18.55	270.2	20.0	136.0	13.13	26.53	0.71	12.70
A32	17.8	16.8	17.29	234.9	20.6	141.0	13.51	24.04	0.74	9.79
A33	18.4	21.3	19.80	307.8	19.8	109.2	12.96	36.10	0.55	22.60
A34	11.7	9.7	10.65	89.1	20.2	151.6	13.21	18.15	0.81	4.13
A36	25.0	21.6	23.24	424.1	19.8	68.8	12.96	35.68	0.30	22.43
A37	16.6	15.7	16.14	204.7	20.3	138.1	13.30	25.52	0.72	11.50
A38	19.1	16.7	17.86	250.5	19.9	141.1	13.04	23.99	0.74	10.21
A39	18.6	16.2	17.36	236.7	20.4	124.6	13.38	31.45	0.64	17.43
A42	22.1	19.6	20.81	340.2	20.2	118.6	13.21	33.57	0.60	19.75
A43	24.1	19.3	21.57	365.3	20.4	114.4	13.38	34.82	0.58	20.87
A45	21.6	20.1	20.84	341.0	20.1	133.5	13.17	27.74	0.69	13.88
A48	20.3	18.1	19.17	288.6	23.8	106.9	15.44	36.60	0.51	20.65
A49	19.9	18.3	19.09	286.3	19.9	119.6	13.04	33.24	0.61	19.58
A50	15.2	14.5	14.85	173.1	3.2	157.5	2.11	14.61	0.95	11.55
A51	23.7	20.3	21.93	377.9	4.9	69.9	3.29	35.92	0.40	32.24
A52	17.8	20.8	19.24	290.8	5.2	126.6	3.51	30.68	0.74	26.43
A53	23.4	20.4	21.85	374.9	5.1	139.8	3.42	24.65	0.83	20.40
A54	24.8	23.4	24.09	455.8	5.2	118.6	3.51	33.57	0.69	29.36
A55	17.0	15.8	16.39	211.0	6.1	152.7	4.10	17.50	0.90	12.50
A56	22.0	18.8	20.34	324.8	5.5	144.4	3.69	22.25	0.85	17.71
A57	12.5	10.6	11.51	104.1	5.1	166.2	3.42	9.09	0.99	4.68
A59	20.3	19.0	19.64	302.9	5.8	127.6	3.92	30.29	0.75	25.62
A60	19.8	18.7	19.24	290.8	5.2	143.3	3.47	22.85	0.85	18.53
A61	16.7	16.2	16.45	212.5	5.3	148.4	3.56	20.02	0.88	15.58
A63	18.4	20.5	19.42	296.3	5.8	152.6	3.87	17.55	0.90	12.78
A64	17.7	22.0	19.73	305.8	5.2	150.2	3.51	19.00	0.89	14.60
A65	23.8	20.4	22.03	381.3	5.2	147.7	3.51	20.42	0.87	16.03
A66	21.0	19.8	20.39	326.6	5.1	130.1	3.42	29.26	0.77	25.07
A67	16.5	14.0	15.20	181.6	5.1	160.0	3.42	13.07	0.95	8.70
A68	23.6	22.1	22.84	409.6	5.6	69.2	3.78	35.72	0.39	31.54
A69	26.3	23.9	25.07	493.7	5.1	68.4	3.42	35.57	0.39	31.76
A70	23.6	21.4	22.47	396.7	5.0	128.2	3.38	30.06	0.75	25.93
A71	17.3	16.8	17.05	228.3	5.0	145.9	3.33	21.43	0.86	17.24

Table 4.10: Cutting energy results for knife-pendulum B

Test #	Minor diameter d	Major diameter D	Equivalent diameter D_{equ}	Cross-section area A	Pendulum starting angle θ_s	Pendulum ending angle θ_e	Pendulum starting energy E_{start}	Pendulum ending energy E_{end}	Energy loss E_{loss}	Cutting energy E_{cut}
	mm	*mm*	*mm*	*mm²*	*deg.*	*deg.*	*J*	*J*	*J*	*J*
B1	17.6	16.6	17.09	229.5	20.1	135.9	13.18	26.59	0.71	12.70
B4	20.4	17.5	18.89	280.4	5.7	150.6	3.83	18.76	0.89	14.04
B5	22.5	20.5	21.48	362.3	5.5	145.4	3.69	21.68	0.86	17.14
B6	18.4	15.8	17.05	228.3	5.5	154.3	3.69	16.59	0.91	11.99
B7	24.8	22.7	23.73	442.1	5.5	118.1	3.69	33.72	0.69	29.34
B11	16.5	19.1	17.75	247.5	5.5	150.3	3.69	18.92	0.89	14.35
B12	16.1	19.2	17.58	242.8	5.4	152.7	3.66	17.52	0.90	12.97
B13	14.0	13.2	13.59	145.1	5.5	161.9	3.69	11.84	0.96	7.20
B14	19.0	17.2	18.08	256.7	5.4	131.6	3.66	28.60	0.77	24.17
B15	20.7	17.5	19.03	284.5	5.3	129.1	3.54	29.68	0.76	25.38
B16	27.1	24.5	25.77	521.5	5.4	56.5	3.66	31.91	0.31	27.94
B17	22.8	18.5	20.54	331.3	5.8	141.0	3.89	24.04	0.83	19.32
B18	20.1	24.0	21.96	378.9	5.4	136.2	3.60	26.46	0.80	22.06
B19	22.4	20.2	21.27	355.4	5.6	126.6	3.77	30.68	0.74	26.17
B20	22.2	19.3	20.70	336.5	5.7	137.2	3.86	25.96	0.81	21.30
B21	20.3	24.6	22.35	392.2	5.7	114.0	3.83	34.93	0.66	30.44
B22	24.2	22.0	23.07	418.1	5.5	117.4	3.69	33.95	0.69	29.58

Average cutting energy values of 18.3 J and 20.4 J for knives A and B, respectively, were observed. Using an ANOVA, it was determined that those values were not significantly different at 5% significance level (Table 4.11). A least significant difference (LSD) of 4.3J applied to the data (Table 4.12).

Table 4.11: ANOVA of stalk cutting energy for treatment (knife) A and B

Source	df	MS	p-value
Knife	1	64.0	0.26
Error	54	50.1	

Table 4.12: Means of stalk cutting energy for knife A and B

	E_c (J)
knife A	18.0
knife B	20.4
LSD (5%)	4.3

Regression analyses were performed to verify the relationship between stalk dimensions (diameter or area) and the cutting energy. A linear relationship was found for the cross-section area with a coefficient of multiple determination of 0.56 and 0.68 for knives A and B, respectively (Figure 4.16 and Figure 4.17).

An attempt was done to plot profiles of the force acting on the knife at each time interval. These measurements would have provided insights into the force pattern during cutting with serrated knifes, which is not a topic well developed in literature. However, this required the calculation of the angular velocity or angular acceleration depending on the method and the differentiation based on discrete intervals did not provide usable results. The use of an accelerometer placed on the knife blade should be used to obtain the adequate data for this type of analysis.

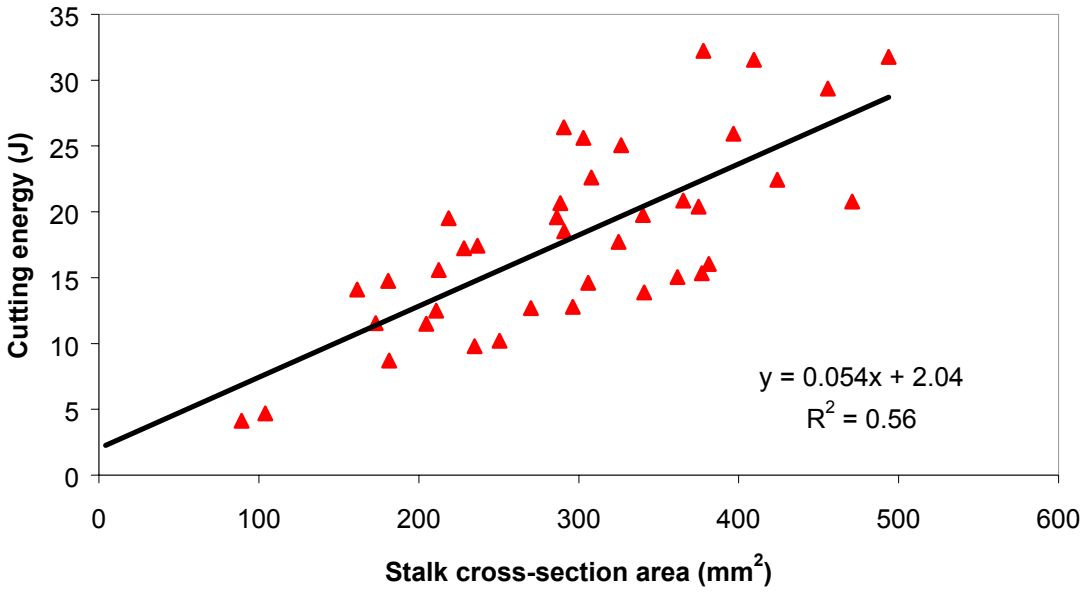

Figure 4.16: Relationship between cutting energy and stalk cross-section area for knife A

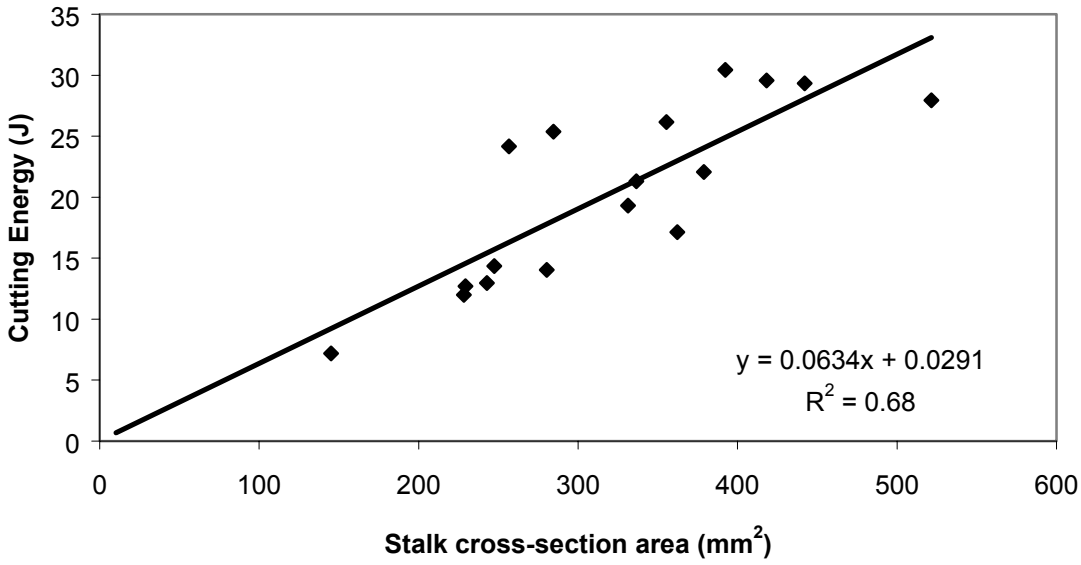

Figure 4.17: Relationship between cutting energy and stalk cross-section area for knife B

The slope of the cutting energy functions found can be seen as area-specific cutting energies. A statistical comparison (t-test) of those energies was done. From the linear regression analysis, the area-specific cutting energy of a given crop specimen was given by:

$$Ec_{ij} = m_j A_i + b_j + e_{ij} \qquad (4.8)$$

for specimen "i" with knife "j".
where

Ec: the cutting energy,
m: the slope of the curve,
A: cross-section area of the stalk,
b: abscissa of the function and
e: error.

The hypotheses were:

H_0: $m_A = m_B$ and
H_1: $m_A \neq m_B$.

The t-value calculated was:

$$t = \frac{m_A - m_B}{\sqrt{S_{m_A}^2 + S_{m_B}^2 + 2\,\mathrm{cov}(m_A, m_B)}} = \frac{0.05401 - 0.06337}{\sqrt{0.007813^2 + 0.01132^2 + 0}} = -0.6805, \qquad (4.9)$$

the degrees of freedom with Satterthwaite's approximation were given by:

$$df = \frac{(S_A + S_B)^2}{\left(\frac{S_A^2}{df_A} + \frac{S_B^2}{df_B}\right)} = \frac{(0.007813 + 0.01132)^2}{\left(\frac{0.007813^2}{39-1} + \frac{0.01132^2}{17-1}\right)} = 38.07 \quad (4.10)$$

and the two-tail t-test with $\alpha = 0.05$ gave:

$t_{0.025,38.07} = 2.33 > t = 0.6805$ (p=0.50)

Therefore, the null hypothesis (H_0) could not be rejected at α=0.05. The slopes, which represent the specific cutting energy for knife A and B, were not statistically different.

4.2.5 Discussion

This experiment allowed the measurement of cutting energy of single corn stalks in conditions similar to field conditions. There was agreement between the literature suggesting that a linear relationship existed between cross-section area and cutting energy for certain crops. For hollow stem plants, the specific cutting energy would be expected to correlate more with diameter. The values obtained in the experiment were larger than those observed in literature. Johnson and Lamp (1966) suggested a cutting energy of 15 J for a 38 mm stalk diameter. Using the relationship developed in this experiment, the cutting energy was estimated to be 72 J for a similar stalk. The non-row sensitive header blades were much thicker than most devices used to measure cutting energy quoted in literature. In fact, the cutting process with thick serrated blades resembled more chipping than pure shearing of the stalk. Moreover, due to the configuration of the apparatus, there was significant friction between the stalk and the blade during cutting. Therefore, the energy measured was not shearing energy but gross or apparent cutting energy. This, however, complies with the objectives to measure cutting energy in the context of a header in field operation or the energy required by the cutting unit.

It should be noted that the specimens used in this experiment were relatively small compared to most conditions encountered in corn silage harvesting. The average stalk

diameter was only ~20 mm while more common values in regions of extended production, such as Québec and Ontario, range between 25 and 30 mm, and even larger in some regions of the United States where the climate is more favourable for corn production and larger varieties. Therefore, the relationship found between cutting energy and stalk cross-section area may not apply to the whole range of corn stalk diameters.

The new generation knife (A) has been designed for a 3.0 m wide header compared to 2.3 m for the previous design, therefore the difference in blade radius. The thinner blade of knife A was designed to reduce the inertia of the machine, the starting loads, and possibly the operating power as well. As shown previously, no significant difference between the required cutting energy was observed. This suggested that the reduced thickness and different blade diameter did not affect greatly the cutting process in this particular configuration. This also suggested that the shape of the knife teeth was probably the main parameter affecting the cutting process. In terms of manufacturing, knife A, which was lower in cost and weight, would be adequate by offering comparable performance as the previous design.

4.2.6 Conclusions on cutting energy experiments

The following conclusions relating to the experimental objectives have been drawn:

- A pendulum apparatus for measuring the cutting energy of corn stalks was successfully built and used to measure the cutting energy of two knives. The knife configurations were compared and found not to be significantly different.
- Average cutting energies measured were 18.0 and 20.4 J for knife A and B, respectively.
- A linear relationship between stalk cross-section area and cutting energy was observed for knives A and B, with R^2 of 0.56 and 0.68, respectively. The slope of the linear functions corresponds to an area-specific cutting energy values that can be used for the modeling of the energy requirements of a non-row sensitive corn header.

4.3 Crushing resistance

4.3.1 Introduction

A second property of corn stalk was measured because no directly applicable data were found in the literature for the proposed analytical model (chapter 5). The crushing resistance or compressive strength of a stalk was defined as the force required to deform its cross-section.

4.3.2 Objectives

The objectives of this experiment were to measure the crushing resistance of the corn stalk at maturity for silage production and develop a relationship between stalk size and resistance.

4.3.3 Material and methods

Randomly selected intact sections of corn stalks used in the cutting energy experiments were cut in lengths of 15-20 cm. The cuts were made outside two stalk nodes in order to maintain the strength and integrity of the specimen. The crushing resistance of 25 specimens was measured using a force displacement apparatus (*Instron model 1011, Instron, Canton, MA*). The specimens were placed horizontally on a 100 mm wide square plate. A 25 mm by 50 mm wide rectangular plate was attached to the moving section of the apparatus. The stalks were compressed with the 25 mm plate side perpendicular to their length (Figure 4.18). A displacement rate of 25 mm per minute was used. Displacement and force were recorded at a rate of 10 Hz. The apparatus was set up to terminate the test when a maximum force of 2250 N was reached to avoid load-cell overload.

The major and minor diameters of the stalk, measured at the test section, were recorded. When proceeding to the test, half the samples were compressed across their major diameter, while the second half of the samples was loaded across their minor diameter.

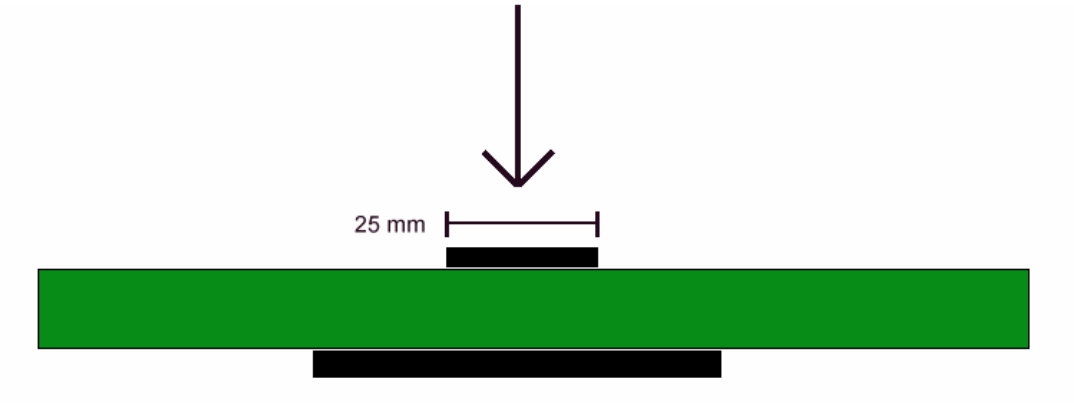

Figure 4.18: Experimental setup for crushing resistance measurements

4.3.4 Results

A data file for each test was obtained containing position and force. The data were formatted and edited to transform the position data into relative deformation by dividing the deformation by the initial diameter. The force-deformation curves showed a similar pattern for all specimens with a quasi-linear relationship up to 50% deformation followed by an exponentially increasing curve approaching full compression (Figure 4.19).

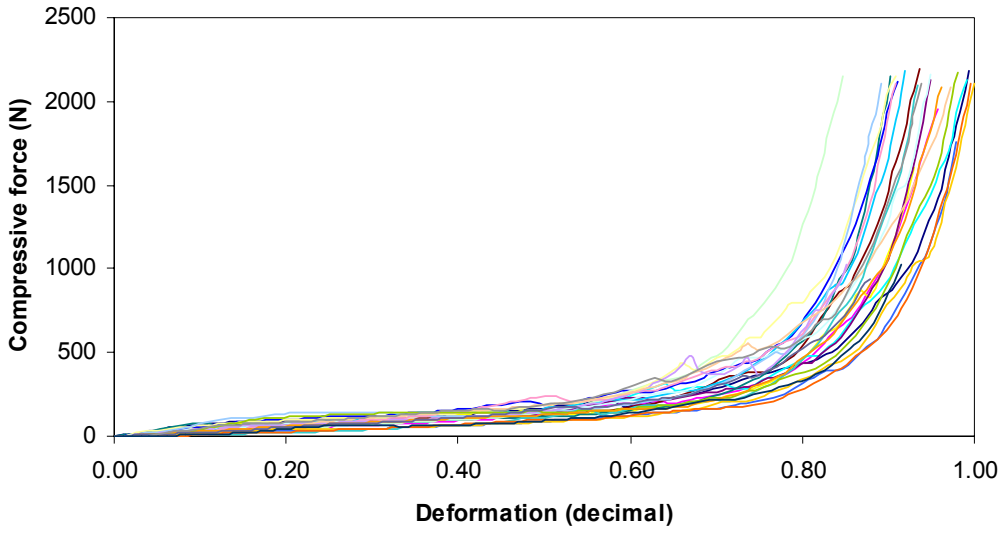

Figure 4.19: Crushing force versus relative deformation measurement of corn stalks cross-section for a 25 mm wide compression width.

Because stalks are only slightly deformed during harvesting, a linear regression was performed on the 0-50% relative deformation range for each sample. The average R^2 of the 25 regressions was 0.91. Figure 4.20 shows an example of regression.

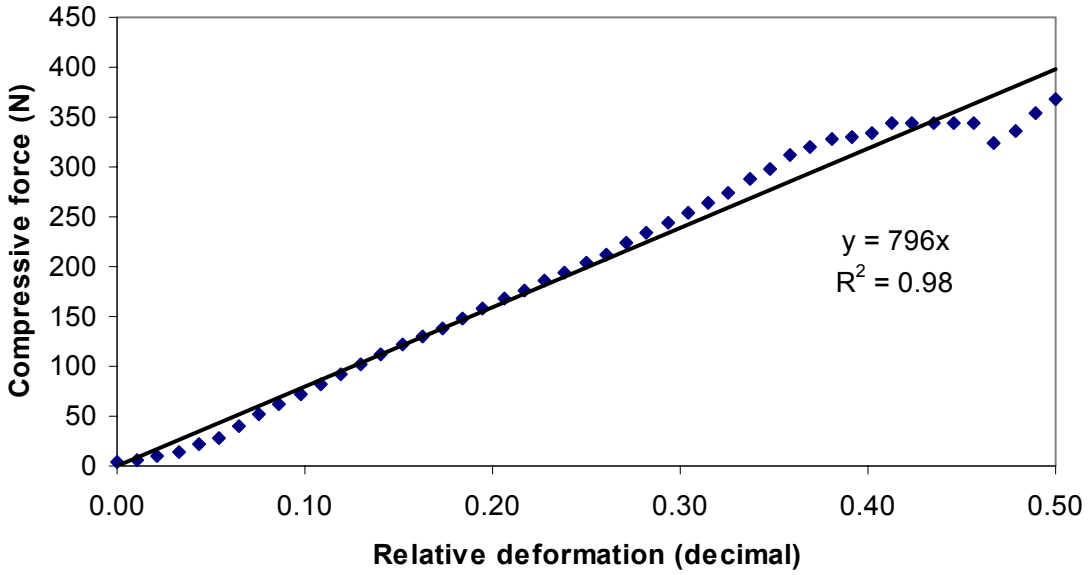

Figure 4.20: Sample of regression of compressive force-deformation curve.

The slopes of the regression curves corresponded to the deformation constant (*K*) investigated. Table 4.13 shows the results of the experiment and the calculated constants. One sample (C13) was rejected due to manipulation errors, reducing the number of tests to 24. The average deformation constant was 6.53 N per percent deformation with a coefficient of variation of 27.7%, which can be consider relatively high.

In order to investigate the stalk size effect, a plot of the slopes (constant *K*) versus the stalk equivalent diameter was created (Figure 4.21). No clear relationship was observed, although *K* was observed to increase with increasing cross-section area. This was expected because the modulus of elasticity of a cylindrical specimen compressed between to parallel plates is a function of the radius of curvature at the contact points (ASAE, 1999). No calculation of the estimated modulii of elasticity have been done,

because they were of little use for this research and required values of properties such as Poisson's ratio, which could not be found for corn stalk.

Table 4.13: Results of compressive resistance experiment

Sample	Major diameter D mm	Minor diameter d mm	Equivalent diameter d_{equ} mm	Cross-section Area mm^2	Deformation constant K (N/% def.)
C1	19.1	17.1	18.1	256.5	7.99
C2	19.0	18.1	18.5	270.1	5.27
C3	19.7	18.4	19.0	284.7	8.11
C4	21.0	17.6	19.2	290.3	5.89
C5	18.8	17.1	17.9	252.5	6.08
C6	17.0	15.6	16.3	208.3	6.48
C7	16.1	15.9	16.0	201.1	6.02
C8	20.6	18.5	19.5	299.3	9.65
C9	19.2	16.3	17.7	245.8	7.96
C10	18.1	15.5	16.7	220.3	6.69
C11	16.8	16.4	16.6	216.4	5.68
C12	19.1	15.7	17.3	235.5	8.48
C14	20.4	16.0	18.1	256.4	8.62
C15	21.8	18.7	20.2	320.2	6.73
C16	19.8	17.3	18.5	269.0	7.98
C17	18.5	16.0	17.2	232.5	3.72
C18	17.3	15.2	16.2	206.5	3.78
C19	17.9	16.8	17.3	236.2	8.67
C20	14.5	15.1	14.8	172.0	3.74
C21	17.9	16.8	17.3	236.2	6.06
C22	17.2	15.5	16.3	209.4	3.82
C23	21.1	18.7	19.9	309.9	6.46
C24	18.8	17.2	18.0	254.0	8.68
C25	20.3	17.2	18.7	274.2	4.17
Average	**18.8**	**16.8**	**17.7**	**248.2**	**6.53**
St. Dev.	**1.74**	**1.14**	**1.34**	**37.2**	**1.81**
C.V.	**0.093**	**0.068**	**0.076**	**0.150**	**0.277**

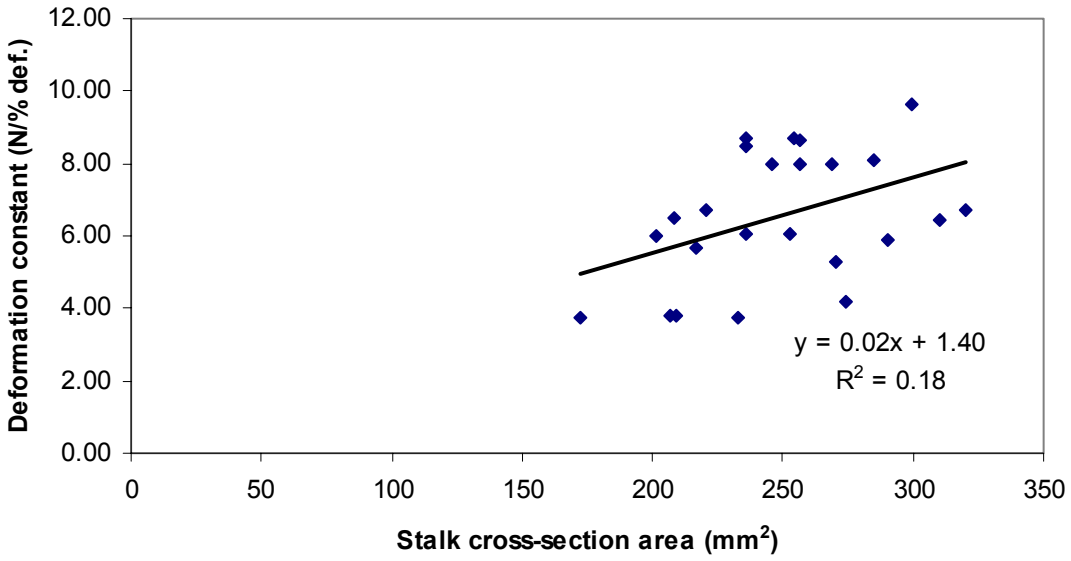

Figure 4.21: Crushing deformation constant versus stalk cross-section area.

4.3.5 Discussion

This experiment provided data on the crushing resistance of corn stalk. The deformation constant calculated for the specimens varied from 4 N/% relative deformation to almost 10 N/%. A very large variability has been observed in the measurements. A larger number of replications would probably give a better correlation between stalk cross-section area and deformation constant. The specimens used ranged in equivalent diameter from 16 to 20 mm. Using the regression formula shown in figure 4.21, a 25 mm stalk equivalent to 490 mm^2 in cross-section area, would have a deformation constant of 11.7 N/%, which is almost 50% greater than for a 20 mm stalk with 8.0 N/%. Because no specimens of this dimension have been tested, extrapolations should be used carefully.

4.3.6 Conclusions on crushing resistance experiments

The following conclusions were made from the experiment on crushing resistance:

- The force-deformation curve of corn stalks cross-section under compressive load was linear up to 50% relative deformation.
- For stalks of diameter ranging from 16 mm to 20 mm, an average deformation constant of 6.53 N per percent of relative deformation was measured.
- No clear correlation between stalk cross-section area and deformation constant were determined although an increasing trend was observed.

4.4 Discussion on experiments

The experiments made for this research provided the data necessary to meet the objectives of modeling the specific energy requirements of a NRS header. Although sufficient replication and randomization was ensured, the conditions and specimens of corn tested may not be representative of the majority. Some important factors that may affect the operation and efficiency of the header were beyond the scope of this research and not accounted for or tested. Those included particularly the condition of the crop in the field which varies from year to year and between regions. The variety of the crop was also not controlled thus the properties measured may not apply reasonably to other varieties grown in other regions, for example. This high level of variability, very common in agriculture, clearly shows the necessity of extensive testing during the development of agricultural machinery. The results of the experiment are, however, a strong basis for the understanding of the processes involved in the non-row sensitive header.

4.5 Conclusions on experiments

In light of the objectives of the experiments, the following conclusions were made:

- Power needs have been measured for a NRS and 3-R header in field conditions and specific energy requirements were calculated. A statistical comparison of the header was made and operating parameters with statistically significant effect were determined.
- The cutting energy of corn stalk for two knife blades was measured. An experimental apparatus was designed and built for that purpose.
- Data on the crushing resistance of stalk was collected to answer the lack of appropriate data in literature.

5. MODELING OF THE SPECIFIC ENERGY REQUIREMENTS A NON-ROW SENSITIVE HEADER

5.1 Introduction

The main objective of this research was to develop models of specific energy requirements in order to predict the power of a NRS header in a given field condition. The models should identify loads to consider in the design and provide insight on means to improve the efficiency.

5.2 Objectives

The objectives of this work were:

- to develop an analytical model based on the analysis of the functions performed by the non-row sensitive header,
- to develop a regression model based on the variables with significant effect on the specific energy of the header from the statistical analysis and
- to apply a general regression model suggested in literature.

5.3 Analytical Model of Specific Energy Requirements

5.3.1 General model

An analytical model was developed to estimate the crop specific energy input required by the prototype harvester, on a dry matter basis. The total power required by the header was categorized in the following operations: free cutting, gathering and conveying. The general form of the model was defined as:

$$SE = \frac{P_0 + P_c + P_g + P_{cv}}{Q(1 - MC)}, \tag{5.1}$$

where:

SE: specific energy of the header (kW·h/Mg),

P_0: no-load power (kW),

P_c: cutting power (kW),

P_g: gathering power (kW),

P_{cv}: conveying power (kW),

Q: mass flow rate (wet basis) (Mg/h) and

MC: crop moisture content (decimal).

For the NRS header, P_0 values were 2.3 kW for the 1000 rpm-800 rpm gearbox and 2.7 kW for the 1000 rpm-1000 rpm gearbox (Section 4.1). For the 3-R header, those values were 1.2 and 1.4 kW, respectively.

5.3.2 Cutting Power

In the proposed model, the cutting power for each disk was calculated based on the work required to cut a single stalk, from the specific cutting energy and the rate at which stalks are cut. The specific cutting energy, E_c, was obtained by experiments as explained in section 4.2 and the cutting power is given by:

$$P_c = \frac{E_c A \dot{p}}{1000} \tag{5.2}$$

where E_c: specific cutting energy (J/mm^2)

A: stalk cross-section (mm^2/plant)

$\dot{p}$: harvesting rate (plants/s)

and the drum harvesting rate is $$\dot{p} = \frac{(Pop)NSV}{10000}, \tag{5.3}$$

where

Pop: corn plant population (plants/ha),

N: number of rows harvested

S: corn row spacing (m) and

V: harvesting speed (m/s).

5.2.3 Gathering Power

Gathering includes the acceleration of the stalks to the drum speed at the moment the stalks are harvested and the work, W_{path} (J) done to move the stalk along the gathering path around the drum (Figure 5.1). The gathering power P_g is defined as:

$$P_g = \dot{p}\frac{\left(\Delta KE + W_{path}\right)}{1000}, \tag{5.4}$$

where ΔKE (J) is the change in kinetic energy of the plant at the point of contact with the drum.

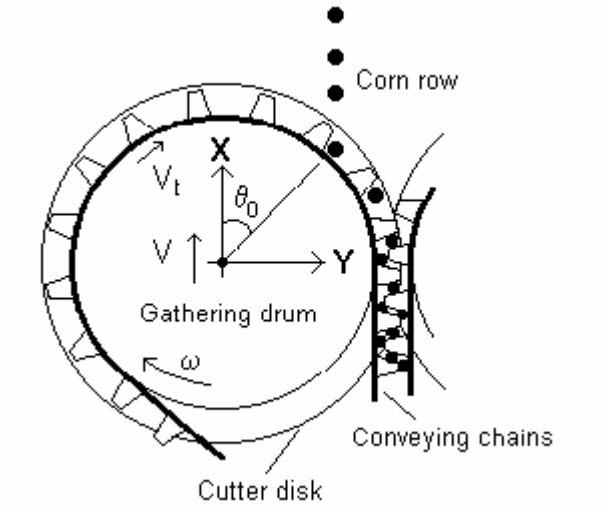

Figure 5.1: General configuration of the non-row sensitive header

The path described by a point on the circumference of a gathering drum of radius *R*, rotating at an angular velocity ω and with a forward velocity *V*, is a cycloid (Bosoi et al., 1991). The angular position, ϕ, of this point after a time *t*, where θ_0 is the initial position of the point with respect to the centre of the drum, along the forward direction ($-\pi/2<\theta_0<\pi/2$) is:

$$\phi = \omega t + \theta_0 . \tag{5.5}$$

Then respective positions in *x* and *y* can be obtained:

$$x(t) = Vt + R\cos\phi = R\left(\frac{V(\omega t)}{\omega R} + \cos\phi\right) = R\left(\frac{\omega t}{\lambda} + \cos\phi\right) \text{ and} \tag{5.6}$$

$$y(t) = R\sin\phi \ , \tag{5.7}$$

where λ is the ratio of the tangential velocity, $V_{t,}$ to the forward velocity, V,

$$(\lambda = \omega R/V = V_t/V). \tag{5.8}$$

For a given drum velocity, the cycloid describing the position of a point on the drum circumference, is contracted at low forward velocities ($\lambda > 1$) and extended at higher forward velocities ($\lambda < 1$) (Figure 5.1).

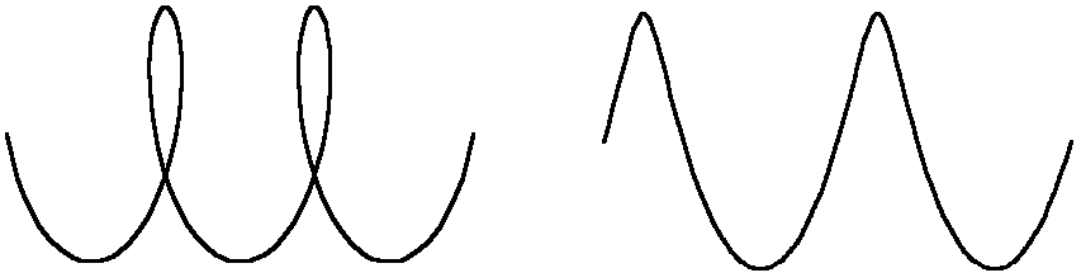

Figure 5.1: Cycloid path for λ =2 (left) and λ =1/2 (right).

The energy input required to move the stalk along the cycloid path comes from two sources. The tractor or propelling element is responsible for the acceleration of the harvested plant to the forward velocity V, therefore the sole energy input from the header consists in the acceleration and transport of the stalk on a circular path, around the drum, up to the delivery point.

During the gathering operation, the stalks are transported by finger-like protrusions on the drums along the gathering path. The weight of the corn stalk is assumed to rest totally on the cutting disk, turning right below the drum at much higher speeds. Therefore, the work to be done (W_{path}) is to overcome the dynamic friction at the bottom of the stalk along the circular path up to the conveying chains. It is given by:

$$
\begin{aligned}
W_{path} &= \int \tau \cdot d\theta \\
&= \int_{\theta_0}^{\pi/2} mg\mu R \cdot d\theta \\
&= mg\mu R\left(\pi/2 - \theta_0\right)
\end{aligned}
\tag{5.9}
$$

where

τ: torque on the drum (N.m),

m: mass of individual corn plant (kg),

g: gravitational acceleration (m/s^2) and

μ: friction coefficient.

Assuming the stalk diameter is much smaller than the blade radius, $d<<R$, the kinetic energy to accelerate the stalk to the velocity of the drum is given by:

$$
\Delta KE_0 = \frac{I\omega^2}{2} = \frac{mR^2\omega^2}{2} = \frac{mV_t^2}{2}. \tag{5.10}
$$

where

V_t : the tangential velocity of the stalk at the drum circumference.

Combining the two terms, the gathering power becomes:

$$
P_g = \dot{p}\left(\Delta KE_0 + W_{path}\right) = \dot{p}m\left[\frac{V_t^2}{2} + \mu gR\left(\pi/2 - \theta_0\right)\right] \tag{5.11}
$$

A friction coefficient, μ, of 0.57 was assumed in the model based on data by Johnson and Lamp (1966) for green corn stalk on sheet metal steel.

As illustrated by equation 5.11, the gathering power depends on the position θ_0. Two cases can be identified:

- In the special case where the direction of harvesting is parallel to the crop rows, θ_0 will take a single value for each row. For example, for the prototype used in the experiments, with a width of 2.21 m, harvesting three rows (0.76 m spacing), the centre row position ranges from θ_0=π/2 rads, when perfectly centred, to θ_0=

0.38 rads at maximum offset (one row is harvested at one extremity of the header) and the others vary similarly.

- If the direction of harvesting is not parallel to crop rows, the harvesting position will be distributed uniformly over the whole width of the header. Then the gathering work is the average work for the whole range of θ_0, which is obtained by setting θ_0=0.

Although there might be significant effects due to the sides of the stalks sliding against the guides, no consideration was given to other sources of friction during the gathering because of the highly unpredictable nature of the process. A more detailed analysis of the trajectory and the contacts of the stalk would be required.

5.3.4 Conveying Power

Conveying power is expressed as the power to transport corn plants along the path of the conveying chains. The conveying load results mostly from the deformation of stalks causing additional friction in the header mechanisms. Because friction forces are usually linear with respect to the normal force applied, the conveying power is assumed to be a linear function of the resulting force from the compression of the stalks. Therefore the conveying power can be expressed as:

$$P_{cv} = \frac{K\delta\mu_o L\dot{p}}{1000}, \tag{5.12}$$

where

δ: Stalk relative deformation of stalks (%), $\delta = \left(\frac{d-s}{d}\right)\times 100$,
s: Spacing between conveying chains (m)
K: Stalk cross–section deformation constant (N / % deformation)
μ_o: Overall friction coefficient
L: Chain conveying length (m)
d: Stalk diameter (m)

A stalk deformation constant of 6.5 N/% deformation was observed in the crushing resistance experiments described previously (Section 4.3), and used in the model.

As seen in equation 5.12, the conveying power is directly proportional to the relative deformation of the corn stalk, δ. Moreover, the value of δ is sensitive to changes in diameter as the latter approaches the value of s. This implies that a good approximation of the stalk diameter is required to evaluate the header power requirements. In the case of stalk diameter approaching or smaller than the chain spacing, the conveying power obtained will approach or be lower than zero, which is not representative of reality. Therefore, the model should not be applied for small stalks, or a minimum conveying power should be estimated from experimental data for this special case.

The friction coefficient μ_o is described as "overall" because it accounts for all friction forces developed by crop flow in the header. Therefore, it is the variable used to fit the model with the experimental data and no theoretical value as been evaluated.

Combining equations 5.2, 5.11, 5.12 and the throughput, $Q = \dot{p}m$, the complete model obtained was:

$$SE = \left(\frac{P_0}{\dot{p}m} + \frac{E_c A}{m} + \frac{V_t^2}{2} + \mu g R\left(\pi/2 - \theta_0\right) + \frac{K\delta\mu_o L}{m} \right)\left(1 - MC\right)^{-1}. \qquad (5.13)$$

5.3.5 Model validation

Using properties measured in laboratory for the cutting energy (Section 4.2) and crushing resistance (Section 4.3), combined with data from literature (e.g. friction coefficient μ), the analytical model was fit to the data from the specific energy measurement experiments (Section 4.1). The only variable unknown that was used to fit the model was the overall friction coefficient, μ_o. With an average corn stalk diameter, *d,* of 26 mm and a chain spacing, *s,* of 20 mm as observed in the field, a value of μ_o of 0.32 was found to optimize the correlation between analytical model values and experimental data with an R^2 of 0.90. This value was considered realistic when considering the geometry of the conveying chain and common steel-steel friction coefficients. Figures 5.2 and 5.3 show the analytical model fit to the specific energy

data measured in the field. The model can not be represented by a line because the average mass of the corn plant is included in the model. With varying yield in the field as measured during the experiment, a related corn plant mass different for each test was obtained.

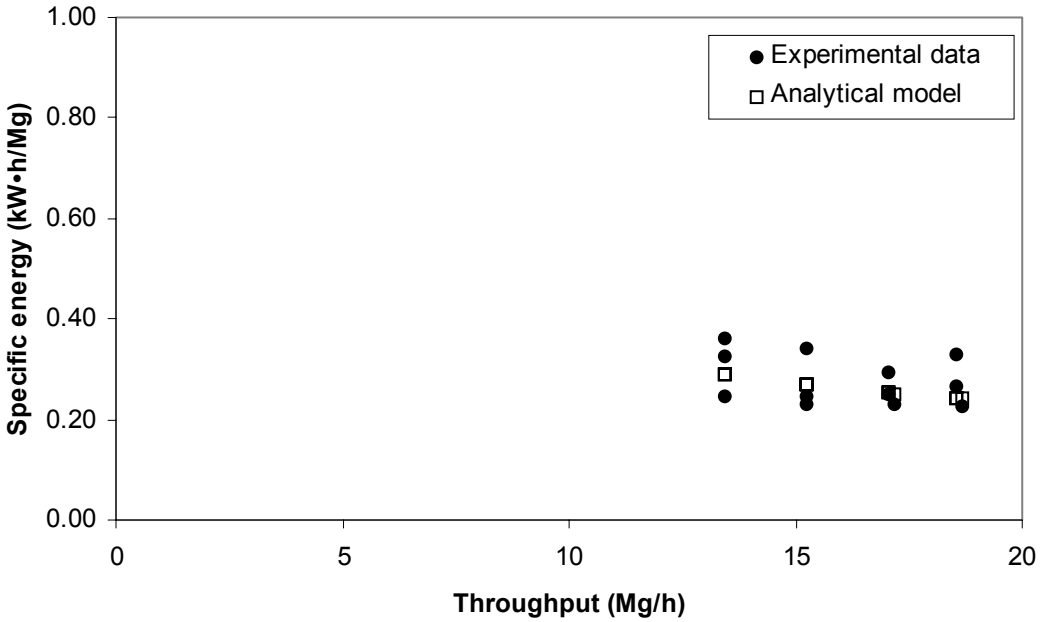

Figure 5.2: Analytical model of specific energy versus experimental data for the 1000-800 gearbox

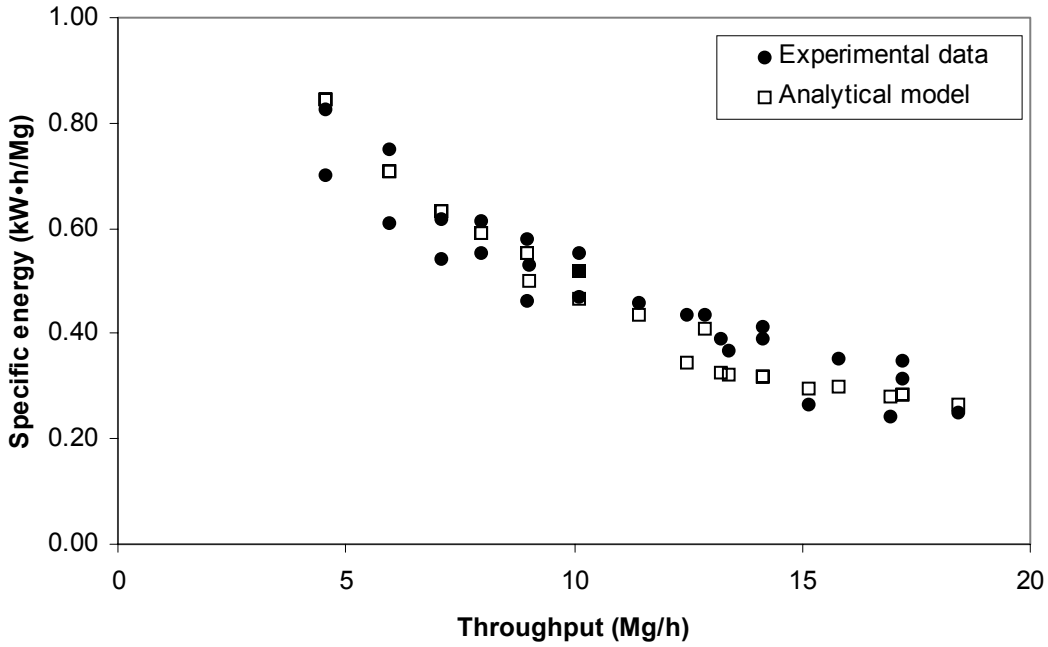

Figure 5.3: Analytical model of specific energy versus experimental data for the 1000-1000 gearbox

5.4 Regression Models

5.4.1 Regression model I

Goering et al. (1993) suggested a model to describe the power requirements of a forage harvester header. This model consisted of a term corresponding to the no-load power and a second term proportional to the throughput,

$$P = C_0 + C_1 Q, \tag{2.4}$$

where

C_0: the no-load power, equal to P_0 (kW),

C_1: constant for any given header (kW.h/Mg) and

Q: the throughput (Mg/h)

Therefore, the specific energy is given by:

$$SE = \frac{C_0}{Q} + C_1 \tag{2.5}$$

This model was fit to the experimental data using different C_0 and C_1 constants for the two header input speed (154 and 123 rpm) with a R^2 of 0.88 (Figure 5.4 and 5.5). The equations obtained were:

$$\begin{aligned} SE &= \frac{2.4}{Q} + 0.13 \qquad \text{for the } 1000\text{-}800 \text{ gearbox} \\ SE &= \frac{2.7}{Q} + 0.20 \qquad \text{for the } 1000\text{-}1000 \text{ gearbox} \end{aligned}, \tag{5.14}$$

where Q and SE are expressed Mg/h and kW·h/Mg DM respectively.

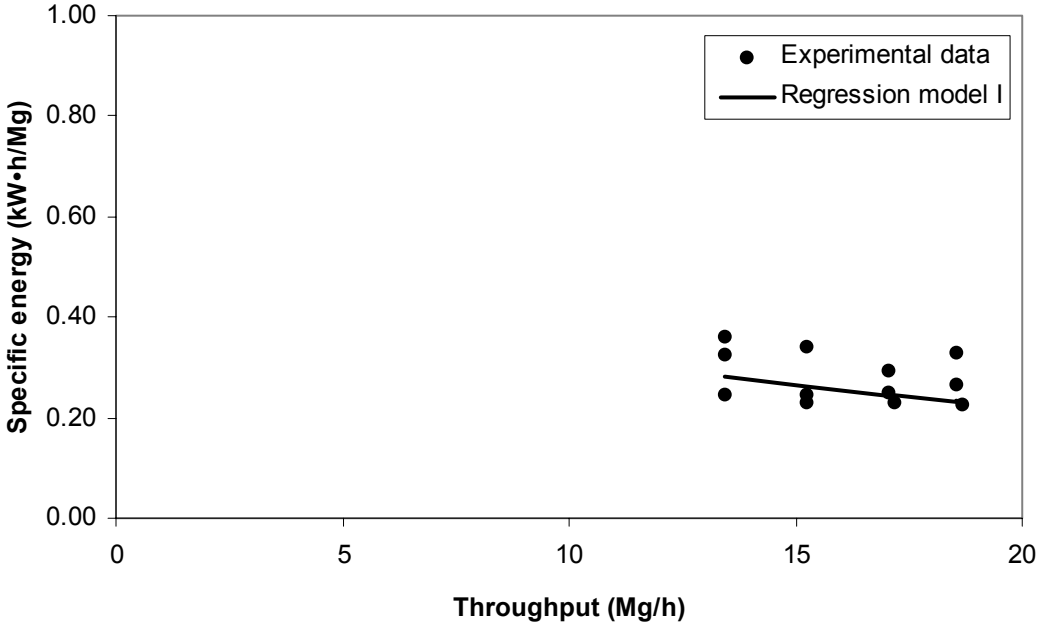

Figure 5.4: Regression model I of specific energy versus experimental data for 1000-800 gearbox

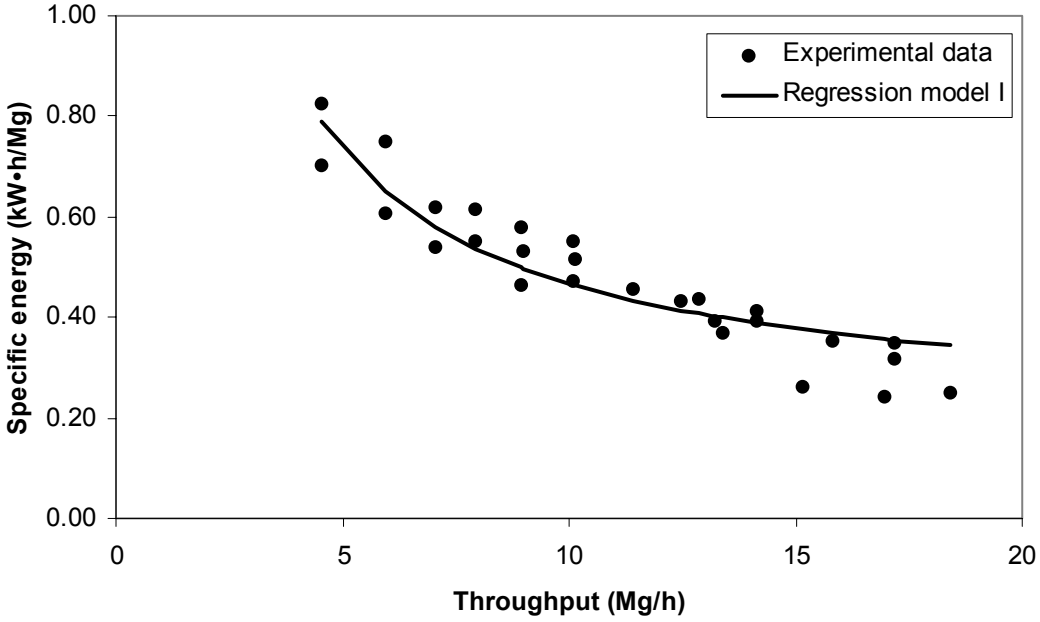

Figure 5.5: Regression model I of specific energy versus experimental data for 1000-1000 gearbox

5.4.2 Regression model II

From the statistical analysis of the experimental specific energy data (Section 4.1) it was concluded that the throughput, Q, and header input speed had an effect on the specific energy of the header. Therefore, a model was developed to include both variables. The input speed was defined as the peripheral velocity V_t of the harvesting drums, in this regression model, which was directly proportional to the header input speed.

To estimate the *SE* under different settings a power-type regression model was obtained:

$$SE = 2.87 \cdot V_t^{1.0} \cdot Q^{-0.66} \tag{5.15}$$

where V_t , Q and *SE* were expressed in m/s, Mg/h and kW·h/Mg on a dry basis, respectively. The model was found to fit the experimental data obtained for the NRS header with a coefficient of multiple determination (R^2) of 0.90 (Figures 5.7 and 5.8). A three-dimensional representation of the model is shown in Figure 5.6.

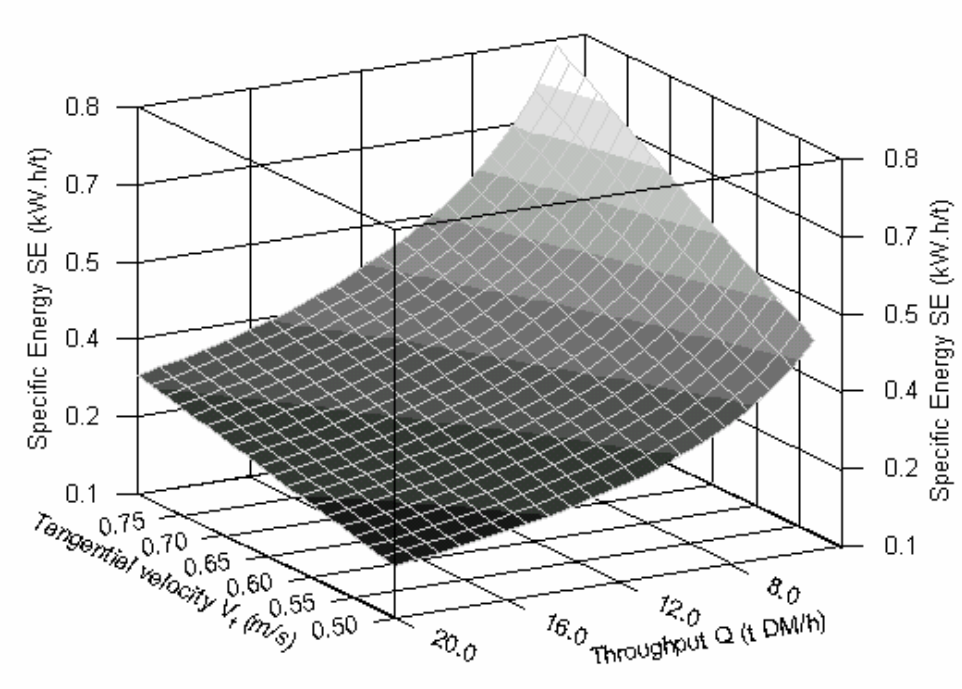

Figure 5.6: Regression model of non-row sensitive header specific energy requirements

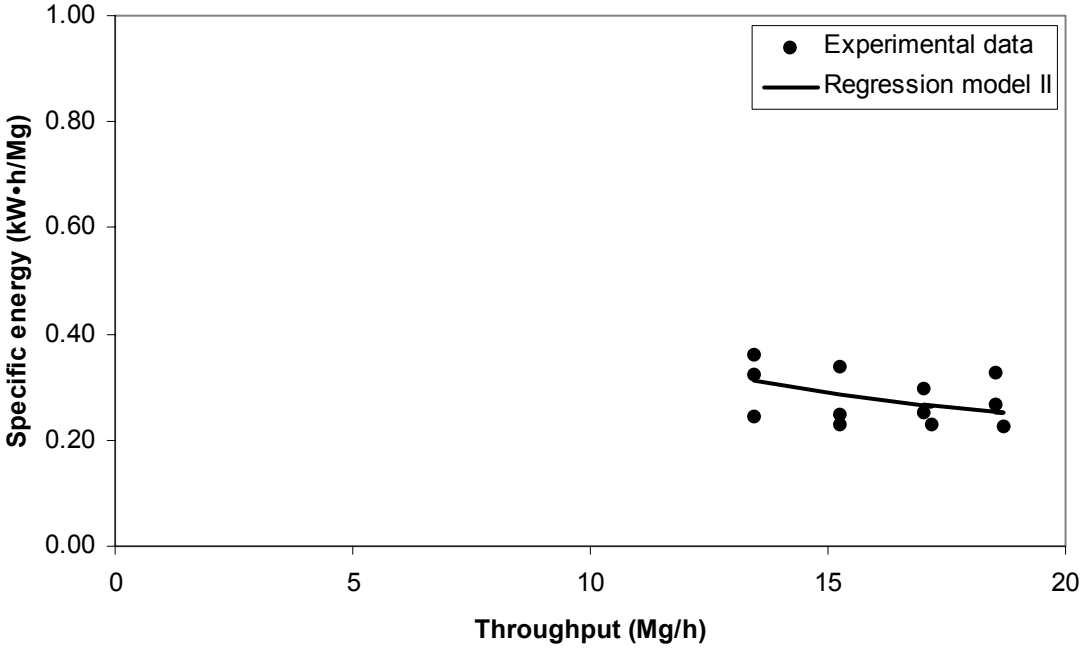

Figure 5.7: Regression model II of specific energy with 1000-800 gearbox

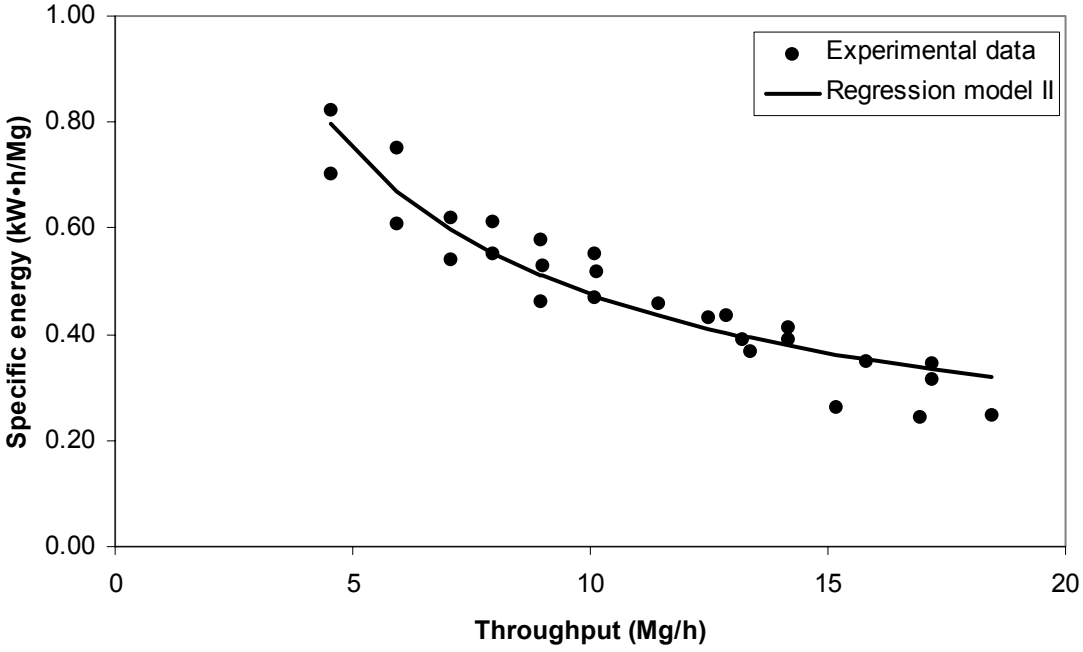

Figure 5.8: Regression model II of specific energy with 1000-1000 gearbox

This model suggested that the specific energy was directly proportional to the header input speed, with an exponent of 1.0. This suggested that the speed of the drum should be kept minimal to reduce power demand, while being able to provide sufficient throughput to accommodate the harvester capacity. The exponent of the throughput, *Q,* in the model differs from the other regression model. The value of –0.66 suggested that the power curve with respect to throughput is not straight as it is suggested by the other two previous models. This causes divergence in the predictions of each model, especially for large throughput values outside the range of validation.

5.5 Specific energy predictions

All three models can be used to obtain estimates or predictions of the specific energy requirements of the non-row sensitive header for given conditions. The analytical model requires several inputs such as the size of the corn stalks, while the regression models only require throughput and the drum peripheral speed. Figure 5.9 shows the specific energy curves for given conditions (80000 plants/ha, 35 Mg/ha yield at 65% moisture content and with 30mm stalk diameter, 1000-1000 gearbox).

Depending on the conditions chosen, the three models give different ranges of predictions. The models tend to diverge with increasing throughput. The data used for the validation covered only values below 20 Mg of dry matter per hour, while the capacity of the machine with the 1000-1000 gearbox can reach almost twice this value when the conditions permit it and sufficient power is available.

Because the models have been validated with limited types of conditions, they can not be directly transferred to any conditions. Taller corn plants or plants with large cobs will have a larger mass, thus provide greater yields, than others of same stalk diameter. This will affect the specific energy required by the header. The regressions models can not be easily applied to different field conditions since they are based solely on field data. Figure 5.10 shows the model applied, as validated in this research, to a field with very low yields (15 Mg/ha), thus a greater mass per plant, while keeping all other

variables unchanged. As it can be seen, the model is largely divergent since the analytical model accounted for a different mass while the regression models did not.

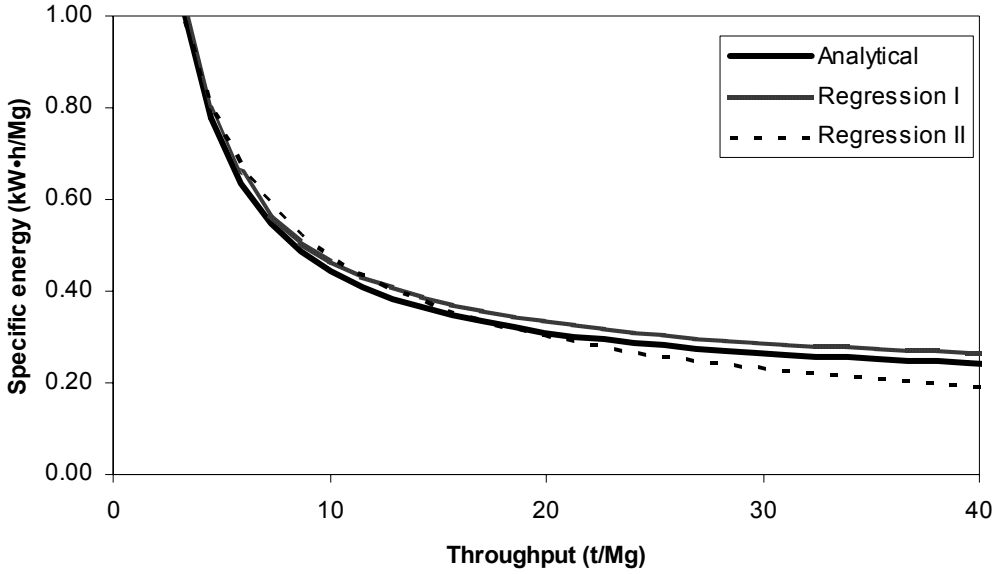

Figure 5.9: Specific energy prediction for three models (80000 plants/ha, 35 Mg/ha yield, 65% moisture content, 30mm stalk, 1000-1000 gearbox).

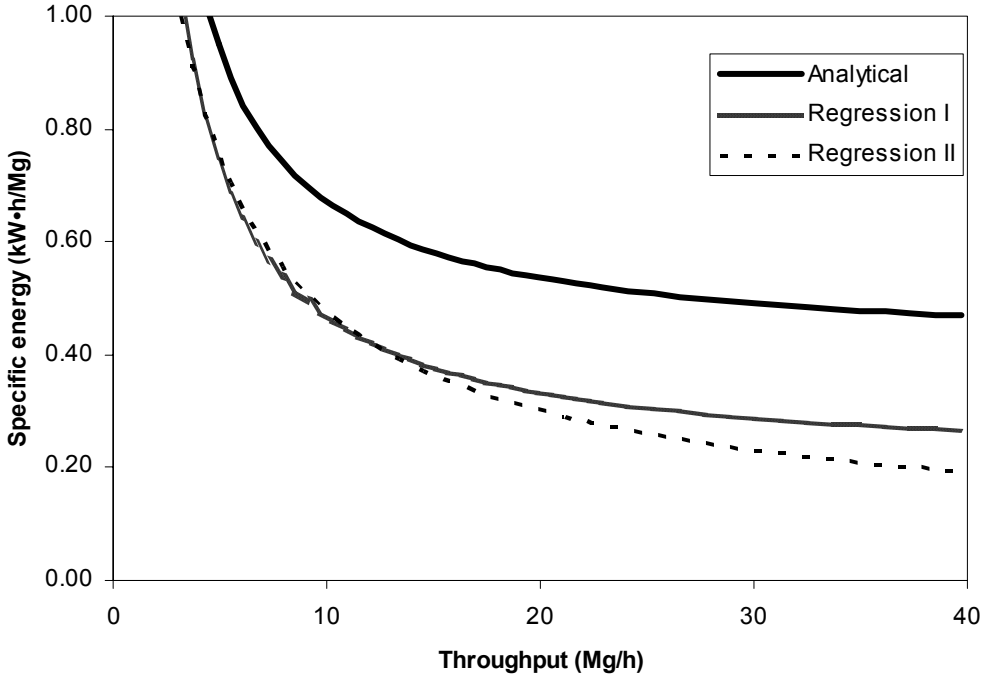

Figure 5.10: Specific energy prediction for three models (80000 plants/ha, 15 Mg/ha yield, 65% moisture content, 30mm stalk, 1000-1000 gearbox).

A second comparison can be made between the models with the same yield as figure 5.8 (35 Mg/ha) but with smaller stalk diameters (24mm) (Figure 5.11). Again the analytical model diverges from the other ones with lower values. Other comparisons could be made to demonstrate the differences between the models. The regression model I shows a direct relationship between the header speed and the specific energy while the regression model II does not account for other header speeds and only one term of the analytical model contains it.

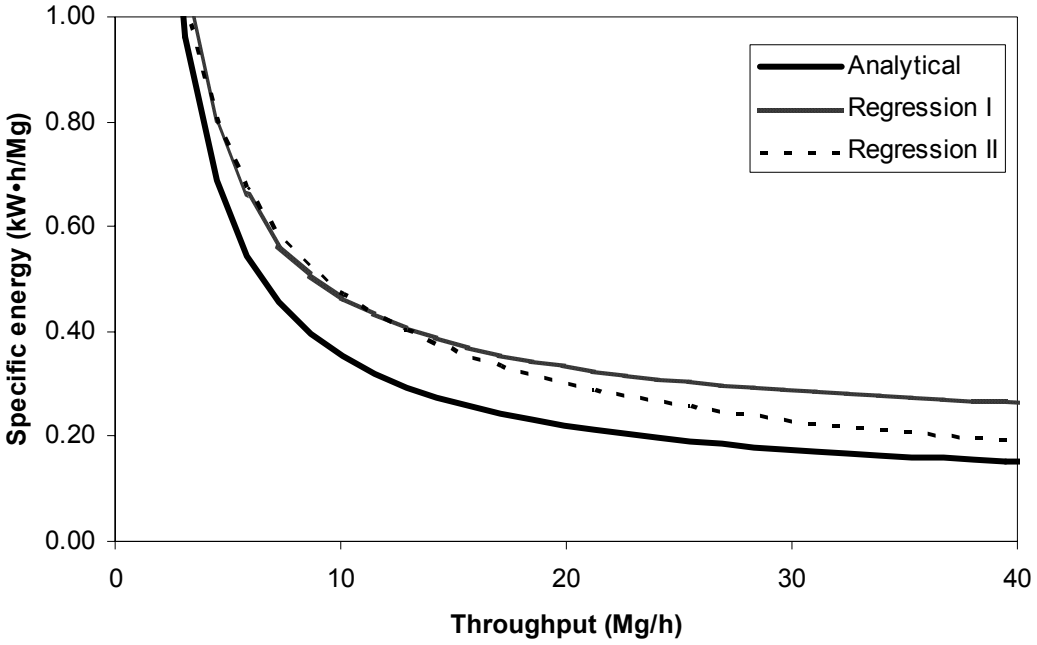

Figure 5.11: Specific energy prediction for three models (80000 plants/ha, 35 Mg/ha yield, 65% moisture content, 24mm stalk, 1000-1000 gearbox).

5.6 Discussion on specific energy models

The comparison of the model equations shows obvious differences and also insights on how to use them and the information they provide. The models can not be used for any

conditions to get an accurate estimation of the specific energy requirements. However, they can be analyzed and compared to study how the specific energy requirements change with different conditions.

The analytical and regression I models suggested a non-zero minimum value of *SE* while the regression model II is asymptotic to zero. Therefore, the models tend to diverge above the range of throughput for which they have been validated. As seen in equation 5.13, the only component of the analytical model which varies with throughput is the term including P_0. This implies a constant "useful" specific energy for given crop conditions and header setting. This is also the case for the regression model I. In fact, the constant, C_1, regroups the terms for cutting, conveying and gathering of the analytical model. However, this variable is valid only for given conditions of crop and harvester settings. For given homogeneous conditions, both models would suggest very similar trends by showing an inverse proportionality between throughput and *SE* requirements or, equivalently, a linear increase in power.

As shown previously, the analytical and the second regression model account for the header speed, V_t. They both suggest an increase in *SE* with increasing speed, although not in the same manner because V_t accounts for a small portion in the analytical model. It must be noticed however, that P_o, the no-load power mostly caused by friction in the moving components, would also change with speed.

According to the analytical model, for conditions similar to those of the experimental tests, the proportions of the *SE* due to no-load, cutting, gathering and conveying power were approximately 50%, 20%, 6% and 24%, respectively. This clearly suggests which function of the header should be optimized.

5.7 Conclusions on specific energy models

One of the main objectives of this research was the development and validation of specific energy models for a non-row sensitive corn header. Three different models were proposed and the following conclusions were made:

- An analysis of the functions performed by the NRS header yielded an analytical model of the specific energy based on the three functions of the header: cutting, gathering and conveying. The model was calibrated and fit with a R^2 of 0.90.
- A model of the specific energy requirements suggested in literature (Goering et al., 1993) was fit to the experimental data with a R^2 of 0.88.
- A regression model based on the throughput and the header working speed was developed and fit to experimental data with a R^2 of 0.90.

6. DISCUSSION & RECOMMENDATIONS

Although the research covered different aspects and variables involved in the operation of the non-row sensitive corn header, the effect of each variable identified, in the analytical model for example, could not be validated due to lack of data and the extensive and varied experiments that it would require. No separate field validation of the model for each of the functions of the header (cutting, gathering and conveying) could be done, although the cutting energy was measured in laboratory. In order to perform this validation, additional measurements on the header would be necessary, i.e. a separate measurement of the load on the cutting blade and the driving components of the conveying chain. It would be very difficult to separate the effect of gathering and conveying because the conveying chains also power the drums which perform the gathering.

The statistical analysis of the experimental specific energy data (Section 4.1) identified two important parameters that affect the required input of energy for harvesting. The throughput and the speed of the header are two variables that can be controlled by the designer and the operator of the machine. The further development of a non-row sensitive header under the concept studied should include trial tests with lower input speeds since they were found to be directly proportional to the power required. The power of the tractor used for harvesting by the farmers may range from 100 to 225 kW, therefore the range of throughput achievable greatly differs. This issue is partially answered by the manufacturer with the two available gearboxes, the 1000-800 rpm for smaller tractors and 1000-1000 rpm for the more powerful tractors. However, further testing is necessary for the optimization of the header speed with respect to the

throughput or capacity required by the header. As seen from the experiments and the models, using the maximum capacity of the tractor by harvesting at the high throughput values, remains the best approach for the operator to increase the efficiency of the header. For large tractors now commonly used with these high-capacity forage harvesters, achieving the optimum throughput levels may become a challenge because of the high working speed involved. Therefore, a wider header covering more area would be necessary to operate at more comfortable speeds (~5-8 km/h).

The literature review and the analysis of the forces involved in the conveying chains also brought useful insight for the improvement of the header power needs. Only minimal force is required to hold the corn plants in place while they are conveyed to the feedrolls. Thus, it would be recommended to increase the spacing between the chains to reduce power needs. A larger space between the chains would also increase the number of stalks that can be held in place for the same length of chain, thereby allowing a further reduction of the chain/drum speed, which was also found to affect the power required. Again, further tests with different chain spacing could identify a more optimum configuration. With the large variety of field conditions that can be encountered over the North American market and over the years, sufficient tests would be necessary to ensure a proper operation in the majority and, ideally, all conditions.

Another point of importance brought up by this research was suggested improvements that could be made to the NRS header design, especially concerning the no-load power, which was found to be about twice the power required by a conventional header of the same width. Moreover, the specific energy needs over the range of throughput evaluated were also consistently higher. Coupled with the high inertia of the moving components, such as the blades and the drums, the high power demand could affect the durability of the forage harvester gearbox that powers the header. The elimination or improvement of the components of the driving mechanisms could improve the concept.

The evaluation of the critical speed for impact cutting of corn, which was found to lie between 6 and 10 m/s for most crop-cutting devices, suggested other possible

improvement to the tested design. The NRS header blade speed was much higher than the critical speed calculated, up to 17.8m/s. Therefore reducing the speed of the blade could help reduce the power requirements. Another alternative would be to reverse the direction of rotation of the cutting disks. The row of fingers on the drum just above the knife would then serve as countershear devices. The presence of countershears dramatically reduces the critical speed of cutting because of the increased bending resistance. Moreover, with the disk and drum turning in opposite direction, their relative speed is increased. Therefore, knife speeds of approximately 10 m/s could be sufficient to cut adequately in the majority of conditions.

Different patterns of knife teeth could also be tested. The two designs tested, with the same teeth profile but different thicknesses, were not statistically different. A thorough study of the knife shape would be necessary.

Finally, the reduction of the specific energy through improvements of the header design should always consider the cost associated and the profitability of the machine for the farmer and for the manufacturer. Small improvements may sometimes cause unnecessary cost increases. The challenge for the engineer or designer remains to find the best compromise between performance and cost.

7. CONCLUSIONS

In the context of the development and testing of a prototype non-row sensitive corn header for a pull-type forage harvester, models to predict the specific energy requirements were developed through the analysis of field data, laboratory experiments and theoretical developments. The model development required particular machine-plant interaction properties to be measured, such as cutting energy and crushing resistance.

The analysis of the field operation of the NRS and 3-R header, the laboratory experiments and the validation of the specific energy models yielded the following conclusions:

- The specific energy requirements of a non-row sensitive header and a conventional three-row header were measured in field conditions. The header type, input speed and throughput were found to have a significant effect on the specific energy requirements. Higher specific energy requirements (0.43 kW·h/Mg) were observed for the non-row sensitive header compared to the conventional one (0.21 kW·h/Mg).

- A model based on the analysis of the cutting, gathering and conveying operations of the header and a regression model based on results of a statistical analysis of the experimental data were developed and validated with the data. A second regression model from the literature was also applied to the field data. All three models were compared with respect to their limits and the information they provide.

- Several recommendations for further tests and improvements of the design of the header were made. Most recommendations aimed at reducing the power requirements of the non-row sensitive header and improve its operation.

REFERENCES

American Society of Agricultural Engineers. 1999. S368.3 Compression test of food materials of convex shape. In *ASAE Standards*, 46th Ed., 570-575. St-Joseph, MI.: ASAE.

American Society of Agricultural Engineers. 1999. S358.2 Moisture Measurements – Forages. In *ASAE Standards*, 46th Ed St-Joseph, MI.: ASAE.

Bagg, Joel. 2001. *Drought damaged corn silage*. Ontario Ministry of Agriculture, Food and Rural Affairs. http://www.gov.on.ca/OMAFRA/english/crops/facts/drought.htm (2003/10/15).

Bosoi, E.S., O.V. Verniaev, I.I. Smirnov and E.G. Sultan-Shakh, 1991. *Theory, Construction and Calculations of Agricultural Machines*, Volume II. Russian Translation Series 83. Rotterdam: Balkema.

Canadian Farm and Industrial Equipment Institute. 2002. CFIEI 2002 Industry Outlook. http://www.cfiei.ca/outlook.html (2002/10/02).

Chancellor, W.J. 1958. Energy requirements for cutting forage. ASAE Paper 58-782. St-Joseph. MI.:ASAE

Figliola, R.S. and D.E. Beasley. 2000. *Theory and Design for Mechanical Measurements*, Third Edition, New York N.Y.: John Wiley and Sons Inc.

Goering, C.E., R.P. Rohrbach and A.K. Srivastava, 1993. *Engineering Principles of Agricultural Machines*, St-Joseph, MI.: ASAE.

Johnson, W.H. and B.J. Lamp, 1966. *Principles, Equipment and Systems for Corn Harvesting*. Wooster, OH: Agricultural consulting associates Inc.

Klenin, N.I., I.F. Popov, V.A. Sakun, 1986. *Agricultural Machines: Theory of Operation,* Computation of Controlling Parameters and the Conditions of Operation. Russian Translation Series 31. Rotterdam: A.A. Balkema.

National Agricultural Statistic Service. 2002. Agricultural Statistics Data Base - USDA-NASS. http://www.nass.usda.gov:81/ipedb/ (2002/10/02).

O'Dogherty, M.J. 1982. A review of research in forage chopping. *Journal of Agricultural Engineering Research*, 27:4, 267-289. National Inst. Agric. Eng., Silsoe, UK.

Persson, S. 1987. *Mechanics of Cutting Plant Material*. St-Joseph. MI.: ASAE.

Sitkei, G. 1986. *Mechanics of Agricultural Materials*. New York: Elsevier.

Shields, J., W. Nawrocki, K.J. Fornstrom and J.L. Smith, 1982. Corn head gathering system performance. ASAE Paper 82-1037. St-Joseph. MI.:ASAE.

Shields, J., W. Nawrocki, K.J. Fornstrom and J.L. Smith, 1984. Variables in forage harvester cornhead gathering system performance. ASAE Paper 84-1529. St-Joseph. MI.:ASAE

Statistics Canada. 2002. Corn silage production. http://datacenter2.chass.utoronto.ca/cgi-bin/cansim2/ (2002/10/01).

APPENDICES

Appendix 1: ANOVA and table of means of specific energy data (experiment #1)

Table A-1: ANOVA of average header specific energy (kW·h/Mg) (Experiment #1).

Source	df	MS	p-value
header	1	0.35458	<.01
Gearbox	1	0.01080	0.02
speed	3	0.00632	0.02
header*gearbox	1	0.00970	0.02
header*speed	3	0.00123	0.53
gearbox*speed	3	0.00063	0.76
header*gearbox*speed	3	0.00068	0.74
Error	30	0.00154	

Table A-2: Means for average header specific energy (kW·h/Mg) (Experiment #1).

Header		
NRS	0.310	
3-R	0.133	
LSD (5%)	0.024	

Gearbox		
1000-1000	0.234	
1000-800	0.209	
LSD (5%)	0.024	

Speed		
1	0.253	a
2	0.224	ab
3	0.200	b
4	0.205	b

Means with same letter are not significantly different at 5% significance level.

Table A-3: ANOVA of maximum header specific energy (kW·h/Mg) (Experiment #1).

Source	df	MS	p-value
header	1	0.5629	<.01
gearbox	1	0.0090	0.06
speed	3	0.0067	0.05
header*gearbox	1	0.0500	<.01
header*speed	3	0.0016	0.57
gearbox*speed	3	0.0012	0.67
header*gearbox*speed	3	0.0017	0.53
Error	30	0.0023	

Table A-4: Means for maximum header specific energy (kW·h/Mg) (Experiment #1).

Header	
NRS	0.392
3-R	0.212
LSD (5%)	0.029

Gearbox	
1000-1000	0.313
1000-800	0.291
LSD (5%)	0.029

Speed	
1	0.337 [a]
2	0.300 [ab]
3	0.281 [b]
4	0.286 [b]

Means with same letter are not significantly different at 5% significance level.

Table A-5: ANOVA of average blower specific energy (kW·h/Mg) (Experiment #1).

Source	df	MS	p-value
header	1	0.597	<0.01
gearbox	1	0.460	0.01
speed	3	0.059	0.36
header*gearbox	1	0.116	0.17
header*speed	3	0.007	0.95
gearbox*speed	3	0.119	0.13
header*gearbox*speed	3	0.022	0.77
Error	30	0.060	

Table A-6: Means for average blower specific energy (kW·h/Mg) (Experiment #1).

Header		
NRS	1.65	
3-R	1.89	
LSD (5%)	0.15	

Gearbox		
1000-1000	1.87	
1000-800	1.67	
LSD (5%)	0.15	

Speed		
1	1.868	a
2	1.786	a
3	1.732	a
4	1.695	a

Means with same letter are not significantly different at 5% significance level.

Table A-7: ANOVA of maximum blower specific energy (kW·h/Mg) (Experiment #1).

Source	df	MS	p-value
header	1	0.6761	0.02
gearbox	1	0.0998	0.35
speed	3	0.1046	0.43
header*gearbox	1	0.1636	0.23
header*speed	3	0.0123	0.95
gearbox*speed	3	0.2818	0.07
header*gearbox*speed	3	0.0348	0.81
Error	30	0.1096	

Talbe A-8: Means for maximum blower specific energy (kW·h/Mg) (Experiment #1).

Header		
NRS	1.74	
3-R	2.00	
LSD (5%)	0.20	
Gearbox		
1000-1000	1.92	
1000-800	1.84	
LSD (5%)	0.20	
Speed		
1	1.990	a
2	1.899	a
3	1.827	a
4	1.773	a

Means with same letter are not significantly different at 5% significance level.

Appendix 2: ANOVA and table of means of specific energy data (experiment #2)

Table A-9: ANOVA of average header specific energy (kW·h/Mg) (Experiment #2).

Source	df	MS	p-value
header	1	0.28862	<.01
speed	5	0.01702	<.01
header*speed	5	0.00098	0.46
Error	22	0.00102	

Table A-10: Means for average blower specific energy (kW·h/Mg) (Experiment #2).

Header	Mean SE	
NRS	0.363	
3-R	0.187	
LSD (0.05)	0.023	

Speed	Mean SE	
1	0.348	a
2	0.304	b
3	0.286	b
4	0.265	bc
5	0.235	cd
6	0.218	d

Means with same letter are not significantly different at 5% significance level.

Table A-11: ANOVA of maximum header specific energy (kW·h/Mg) (Experiment #2).

Source	df	MS	p-value
header	1	0.6801	<.01
speed	5	0.0254	<.01
header*speed	5	0.0035	0.23
Error	22	0.0023	

Table A-12: Means for maximum header specific energy (kW·h/Mg) (Experiment #2).

Header	Mean SE	
NRS	0.496	
3-R	0.224	
LSD (0.05)	0.034	

Speed		
1	0.438	a
2	0.384	ab
3	0.352	b
4	0.363	b
5	0.310	bc
6	0.285	c

Means with same letter are not significantly different at 5% significance level.

Table A-13: ANOVA of average blower specific energy (kW·h/Mg) (Experiment #2).

Source	df	MS	p-value
header	1	0.2759	0.07
speed	5	0.1526	0.12
header*speed	5	0.0803	0.42
Error	22	0.0776	

Table A-14: Means for average blower specific energy (kW·h/Mg) (Experiment #2).

Header	Mean	SE
NRS	1.64	
3-R	1.49	
LSD (0.05)	0.20	

Speed		
1	1.806	a
2	1.588	ab
3	1.485	ab
4	1.675	ab
5	1.422	b
6	1.438	b

Means with same letter are not significantly different at 5% significance level.

Table A-15: ANOVA of maximum blower specific energy (kW·h/Mg) (Experiment #2).

Source	df	MS	p-value
header	1	1.172	<0.01
speed	5	1.020	<0.01
header*speed	5	0.651	<0.01
Error	22	0.146	

Table A-16: Means for maximum blower specific energy (kW·h/Mg) (Experiment #2).

Header	Mean	SE
NRS	2.30	
3-R	2.03	
LSD (0.05)	0.27	

Speed		
1	2.990	a
2	2.397	ab
3	1.958	bc
4	2.295	b
5	1.865	bc
6	1.805	c

Means with same letter are not significantly different at 5% significance level.

Appendix 3: ANCOVA and table of means of specific energy data (experiment #1)

Table A-17: ANCOVA of average header specific energy (kW·h/Mg) (Experiment #1)

Source	df	MS	p-value
Header	1	0.37328	<.01
Gearbox	1	0.00908	0.01
Header*Gearbox	1	0.00804	0.02
Q	1	0.02107	<.01
Error	30	0.00132	

Table A-18: Means for average header specific energy (kW·h/Mg) (Experiment #1)

Header	
NRS	0.310
3-R	0.133
LSD (0.05)	0.024

Gearbox	
1000-1000	0.234
1000-800	0.209
LSD (0.05)	0.024

Table A-19: ANCOVA of maximum header specific energy (kW·h/Mg) (Experiment #1)

Source	df	MS	p-value
Header	1	0.3835	<.01
Gearbox	1	0.0077	0.05
Header*Gearbox	1	0.0453	<.01
Q	1	0.0212	<.01
Error	41	0.0020	

Table A-20: Means for maximum header specific energy (kW·h/Mg) (Experiment #1)

Header	
NRS	0.392
3-R	0.212
LSD (0.05)	0.029

Gearbox	
1000-1000	0.313
1000-800	0.291
LSD (0.05)	0.029

Table A-21: ANCOVA of average blower specific energy (kW·h/Mg) (Experiment #1)

Source	df	MS	p-value
Header	1	0.613	<0.01
Gearbox	1	0.376	0.01
Header*Gearbox	1	0.098	0.19
Q	1	0.199	0.06
Error	41	0.054	

Table A-22: Means for average blower specific energy (kW·h/Mg) (Experiment #1)

Header	
NRS	1.65
3-R	1.89
LSD (0.05)	0.15

Gearbox	
1000-1000	1.87
1000-800	1.67
LSD (0.05)	0.15

Table A-23: ANCOVA of maximum blower specific energy (kW·h/Mg) (Experiment #1)

Source	df	MS	p-value
Header	1	0.7049	0.01
Gearbox	1	0.0525	0.48
Header*Gearbox	1	0.1335	0.27
Q	1	0.3004	0.10
Error	41	0.1046	

Table A-24: Means for maximum blower specific energy (kW·h/Mg) (Experiment #1)

Header	
NRS	1.74
3-R	2.00
LSD (0.05)	0.20

Transmission	
1000-1000	1.92
1000-800	1.84
LSD (0.05)	0.20

Appendix 4: ANCOVA and table of means of specific energy data (experiment #2)

Table A-25: ANCOVA of average header specific energy (kW·h/Mg) (Experiment #2)

Source	df	MS	p-value
Header	1	0.21772	<.01
Q	1	0.08240	<.01
Error	31	0.00087	

Table A-26: Means for average header specific energy (kW·h/Mg) (Experiment #2)

Header	
NRS	0.363
3-R	0.187
LSD (0.05)	0.023

Table A-27: ANCOVA of maximum header specific energy (kW·h/Mg) (Experiment #2)

Source	df	MS	p-value
Header	1	0.54915	<.01
Q	1	0.13209	<.01
Error	31	0.00187	

Table A-28: Means for maximum header specific energy (kW·h/Mg) (Experiment #2)

Header	Mean SE
NRS	0.496
3-R	0.224
LSD (0.05)	0.034

Table A-29: ANCOVA of average blower specific energy (kW·h/Mg) (Experiment #2)

Source	df	MS	p-value
Header	1	0.0938	0.25
Q	1	0.7044	0.00
Error	31	0.0668	

Table A-30: Means for average blower specific energy (kW·h/Mg) (Experiment #2)

Header	Mean SE
NRS	1.64
3-R	1.49
LSD (0.05)	0.20

Table A31: ANCOVA of maximum blower specific energy (kW·h/Mg) (Experiment #2)

Source	df	MS	p-value
Header	1	0.238	0.30
Q	1	4.081	<0.01
Error	31	0.212	

Table A-32: Means for maximum blower specific energy (kW·h/Mg) (Experiment #2)

Header	Mean SE
NRS	2.30
3-R	2.03
LSD (0.05)	0.27

Appendix 5: Calibration and friction losses calculation for cutting energy measurement apparatus.

Table A-33: Potentiometer calibration for angular position versus output voltage

Test #	Angle (^{o})	mV
A-90	90	1252
A-20	20	220
A-160	160	2283
B-90	90	1244
B-20	20	220

Calibration equation:
Angle = 0.0679*(mV) + 5.13
(R^2=0.99)

Table A-34: No-cut sample tests for determination of energy losses due to friction

	Starting angle θ_{start}	*Ending angle* θ_{end}	*Starting energy* E_{start}	*Ending energy* E_{end}	*Energy loss* E_{loss}	*Energy loss* E_{loss}*/deg.*
Test #	*degrees*	*Degrees*	*J*	*J*	*J*	*J/deg.*
A-a	19.93	159.40	25.21	24.79	0.42	0.0030
A-b	20.00	158.96	25.17	24.52	0.65	0.0047
A-c	19.66	159.01	25.38	24.55	0.83	0.0060
A-d	5.07	173.19	34.87	33.72	1.16	0.0069
A-e	4.93	172.75	34.96	33.42	1.54	0.0092
A-f	5.88	172.35	34.33	33.16	1.17	0.0070
					Average	0.00613
					St. Dev.	0.00212
B-a	20.11	157.62	25.10	23.69	1.41	0.0103
B-b	20.16	157.55	25.07	23.64	1.42	0.0104
B-c	20.16	157.62	25.07	23.69	1.38	0.0100
B-d	5.53	172.35	34.56	33.16	1.41	0.0084
B-e	5.53	172.29	34.56	33.12	1.45	0.0087
B-f	5.53	171.88	34.56	32.85	1.72	0.0103
					Average	0.00968
					St. Dev.	0.00089